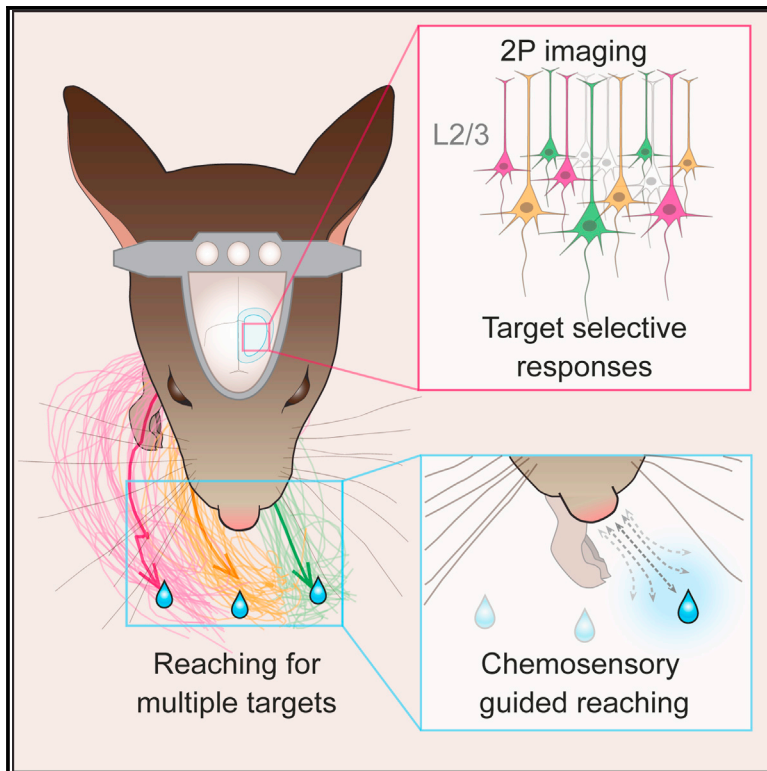# Cell Reports

Directional Reaching for Water as a Cortex-Dependent Behavioral Framework for Mice

Graphical Abstract

Authors

Gregorio Luis Galiñanes, Claudia Bonardi, Daniel Huber

Correspondence

daniel.huber@unige.ch

In Brief

Galiñanes et al. present a behavioral framework for systems neuroscience in which mice learn to reach for water droplets presented at multiple locations, similar to the primate center-out task. Reaching is guided by chemosensory cues and depends on motor cortex. Layer 2/3 neurons display a high degree of directional selectivity.

Highlights

- Mice rapidly learn to reach for water droplets in multiple directions using chemosensation

- Directional reaching can be instructed by arbitrary sensorimotor associations

- Optogenetic motor cortex silencing halts movement initiation and ongoing reaching

- Motor cortex layer 2/3 neurons display a high degree of directional selectivity

CellPress

Directional Reaching for Water as a Cortex-Dependent Behavioral Framework for Mice

Gregorio Luis Galiñanes,[1,2] Claudia Bonardi,[1,2] and Daniel Huber[1,3,*]
[1]Department of Basic Neurosciences, University of Geneva, Geneva, Switzerland
[2]These authors contributed equally
[3]Lead Contact
*Correspondence: daniel.huber@unige.ch
 https://doi.org/10.1016/j.celrep.2018.02.042

SUMMARY

Optogenetic tools and imaging methods for recording and manipulating brain activity have boosted the field of neuroscience in unprecedented ways. However, behavioral paradigms for mice lag behind those of primates, limiting the full potential of such tools. Here, we present an innovative behavioral framework in which head-fixed mice directionally reach for water droplets, similar to the primate "center-out" reaching task. Mice rapidly engaged in the task, performed hundreds of trials, and reached in multiple directions when droplets were presented at different locations. Surprisingly, mice used chemosensation to determine the presence of water droplets. Optogenetic inactivation of the motor cortex halted the initiation and rapidly diverted the trajectory of ongoing movements. Layer 2/3 two-photon imaging revealed robust direction selectivity in most reach-related neurons. Finally, mice performed directional reaching instructed by vibrotactile stimuli, demonstrating the potential of this framework for studying, in addition to motor control, sensory processing, and decision making.

INTRODUCTION

Reaching toward a target and manipulating objects are motor behaviors that dominate many aspects of our daily lives. They require complex computations of target location, body position, motor planning, preparation, and execution. The underlying neuronal correlates have been extensively studied in primates using confined experimental conditions designed for precise limb tracking, defined stimulus control, and stable neuronal recordings. The classic "center-out" task consists of a visually cued directional movement of the forearm from an initial position toward one of multiple targets located in a plane (Georgopoulos et al., 1982) or in three dimensions (Schwartz et al., 1988). This type of directional reaching paradigm has not only allowed the development of important concepts about population coding (Georgopoulos et al., 1986), motor planning, mental rehearsal,

decision making (Cisek and Kalaska, 2004, 2005), and neuro-prosthetic control (Taylor et al., 2002), but also offered the basis for computational frameworks, necessary to causally link neuronal activity with motor control (Scott and Kalaska, 1997; Shadmehr and Mussa-Ivaldi, 1994). Cue-guided, delayed, and memory-based versions of this task have made it possible to probe different aspects of sensory-motor processing.

With the recent development of genetic and viral tools, as well as optical imaging and electrophysiological techniques, more experimental work has shifted toward the mouse for investigating sensory-motor transformations (O'Connor et al., 2009) and dissecting neural circuits controlling behavior (Luo et al., 2008). It is therefore essential to develop well-controlled behavioral paradigms suited for head-fixed mice that, at the same time, have ethological and translational value. Until today, such paradigms in rodents remain below the gold standard of primate behavior. For instance, joystick or lever tasks emulating human behavior have been developed for mice, yet most of them constrain the behavioral repertoire to pull or push movements (Hira et al., 2013; Morandell and Huber, 2017; Peters et al., 2014). Similarly to primates, rodents perform forelimb skilled movements for manipulating and reaching objects, which share many common traits with those of primates. Indeed, the close resemblance of the reach-to-grasp sequence supports the hypothesis that reaching behavior is homologous in rodents and primates (Sacrey et al., 2009; Whishaw et al., 1992) and has led to the development of widely used food pellet reaching tasks for rats and mice. Moreover, rodent models of Parkinson's disease, Huntington's disease, and stroke display impairments in reaching performance similar to human patients. Skilled reaching for food pellets has therefore been proposed as a translational tool for investigating neurological diseases (for a review, see Klein et al., 2012) and is widely used to study motor skill learning (Chen et al., 2014; Harms et al., 2008; Kleim et al., 2004; Xu et al., 2009).

However, compared with the "center-out" reaching task in primates, reaching for pellets in mice currently has several limitations, and its use under head-fixed conditions is only emerging (Guo et al., 2015; Whishaw et al., 2017). Pellet reaching in rodents is typically limited to a single target, and the location and availability of the pellet are detected by its odor (Whishaw and Tomie, 1989). These factors preclude the separation of the sensory and motor responses hampering dissection of neuronal

activity related to movement direction, motor planning, working memory, or arbitrary sensorimotor mappings. As a consequence, the transfer to computational frameworks for motor control in mice is limited. Also, the relatively large reward size leads to a small number of repetitions per session (<50 trials; Esposito et al., 2014; Guo et al., 2015; Wang et al., 2017; Xu et al., 2009), thus reducing statistical power. Movement artifacts and myoelectric potentials (Sasaki et al., 1983) caused by chewing of compressed food pellets can furthermore interfere with electrophysiological and optical recordings, compromising the quality of neurophysiological data. Finally, high-throughput automatization of pellet placement and scoring of success rate requires complex mechanics and advanced video tracking systems (Ellens et al., 2016; Guo et al., 2015; Wong et al., 2015). In contrast, other head-fixed behavioral paradigms for mice, which use licking as a motor output, rely on liquid rewards and thereby circumvent many of these issues, reducing chewing artifacts, allowing hundreds of repetitions and simplifying the liquid reward delivery with valves (Guo et al., 2014a). However, the translational value of such tasks for studying motor systems is limited.

To overcome the limitations of existing behavioral tasks, we propose a directional reaching paradigm combining the reach-to-grasp movement and convenience of water-based training in mice, with the multi-directionality and cue-guided principles of the primate "center-out" task. Our results show that reaching for water is quickly learned and easily implemented; yet it can be adapted from low- to high-level complexity settings, reproducing most of the hallmarks of the "center-out" task. We found that head-fixed mice use a chemosensory system to locate water droplets, that reaching is strongly affected by motor cortex inactivation, that layer 2/3 neurons of the motor cortex display direction-selective responses, and that arbitrary stimuli can be associated with different target locations. We thus provide a promising framework with potential for studying sensorimotor processing as well as instructed motor behavior and decision making in mice.

RESULTS

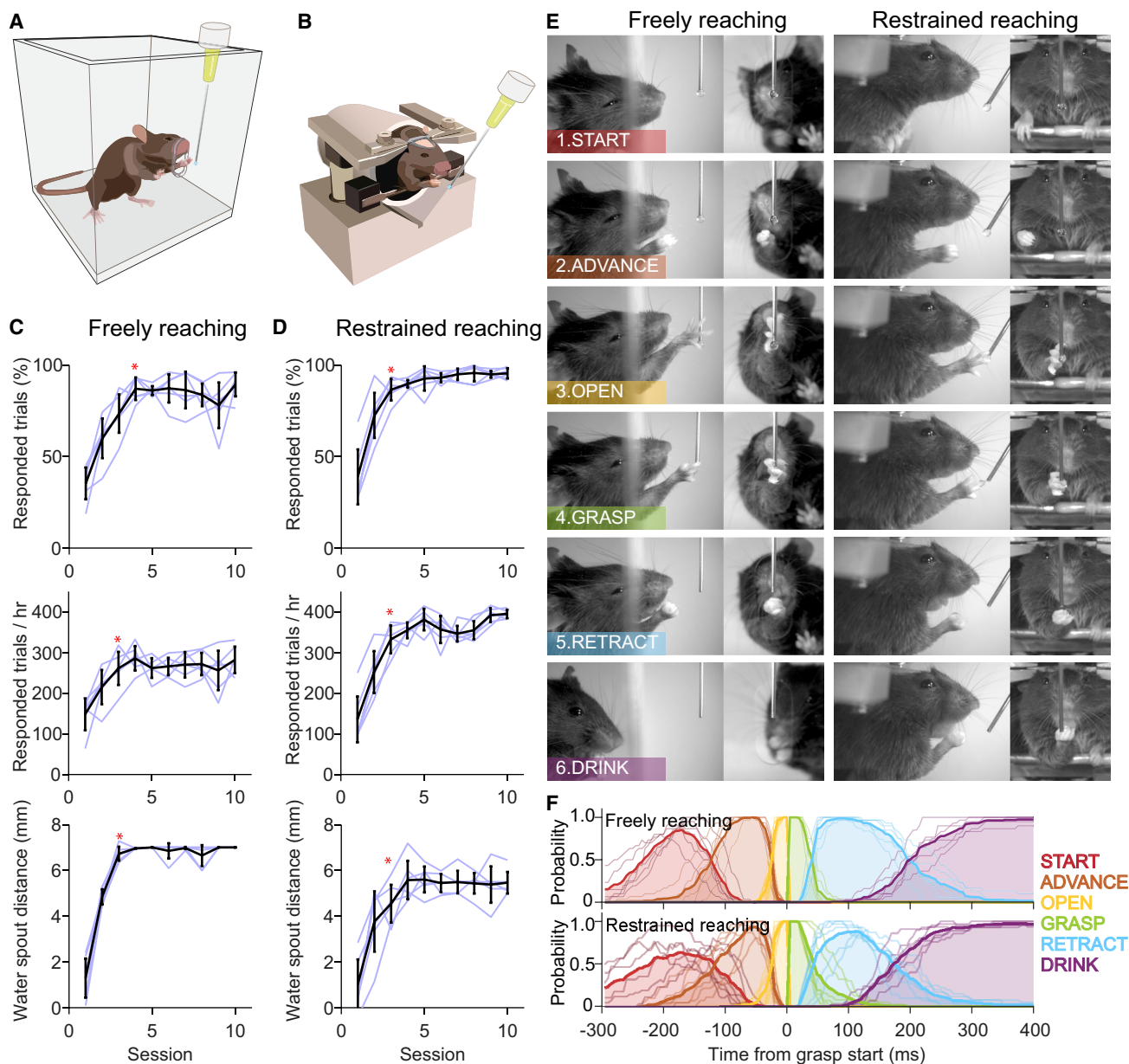### Mice Rapidly Learn to Reach for Water Droplets

Water rewards are well suited to motivate mice to participate in behavioral experiments under head-fixed conditions. Water-deprived mice readily produce hundreds of trials per session in which rewards are usually collected by licking (Guo et al., 2014a). Also, rodents are proficient at reaching and manipulating objects, making the reach-to-grasp behavior an attractive motor output because of its translational value. A behavioral task in which mice reach and grasp for water rewards would combine the best of both approaches.

To test this idea, we trained water-deprived mice to reach for water droplets in an acrylic glass chamber (10 × 10 × 10 cm) with a slit in one of the walls, allowing the mice to protrude their snout or forelimb (Figure 1A). A water spout outside the chamber supplied ~5 μL droplets of water that were signaled with a "beep" sound. Mice freely explored the chamber and licked the water spout within 5.5 ± 2.6 water drop deliveries (trials). Surprisingly, even though the water spout was at licking distance (Figure S1A), mice spontaneously performed reach-to-grasp

movements to collect and consume the water droplets (after 4.3 ± 3 collected rewards through licking). To favor the reach-to-grasp behavior, the water spout was gradually moved farther away, and all mice completely switched to reaching behavior during the first session. Over the course of the following training sessions, the distance of the water spout was further increased to its final position at 7 mm from the tip of the snout. Training session duration was limited to ~30 min to make learning rates comparable with published pellet reaching training paradigms (Chen et al., 2014). By the fourth session, animals were already engaged in the task, responding in $87.4 \pm 6.8\%$ of 166 ± 17 trials per session (32.6 ± 2.22 min session duration, 282 ± 35 reached trials/hr; Figure 1C). At the end of the session, mice were still actively engaged in the task and not satiated (0.55 ± 0.05 mL of water drunk during the session). This was confirmed in a session with no time limit (Experimental Procedures), in which mice were engaged in the task for at least 60 min, collected a total of 1.03 ± 0.21 mL, and responded in 438 ± 60 trials (Figure S1B). Trials without a response were typically due to the mice grooming or exploring the chamber and rarely due to failing to reach the water droplet. On the contrary, mice performed "in-vain" reaches (i.e., reaching movements toward the target before reward presentation; Figure S1C; Chen et al., 2014), suggesting an exploratory strategy and behavioral engagement.

Next, we examined whether mice were able to perform the same task in the head-fixed condition (Figure 1B). They were trained similarly to freely reaching mice and engaged in the task attaining plateau performance levels by the third session (Figure 1D). Although freely reaching mice spent time grooming and exploring the arena, restrained mice seemed to be more focused on the task, responding in $89.7 \pm 2.8\%$ of 200 ± 7.9 trials by the fourth session (30.5 ± 0.6 min duration, 354 ± 22 reaches/hr; Figure 1D). Head-fixed mice also performed fewer "in-vain" reaches per trial after the fourth session ($p < 0.01$, Tukey post hoc test, after significant interaction of repeated-measures ANOVA; Figure S1C). Thus, reaching for and grasping water droplets is a behavioral task that mice adopt in a few sessions under both freely moving and head-fixed conditions.

We compared the sequence of the reach-to-grasp movements in freely moving and head-fixed settings and found similar dynamics (Figures 1E and 1F; Movies S1 and S2). In both conditions, mice first moved the paw to an initial position (START) supinating the paw, flexing the digits, and aiming the target. Once the target was aimed, the forelimb was moved toward it (ADVANCE). At the end of the advance phase, digits were opened and extended (OPEN), and the paw adducted toward the target. The grasping movement was typically initiated upon touching the target (GRASP) and followed by supination of the paw and retraction of the arm toward the mouth (RETRACT) for water drop consumption (DRINK). The average duration of a complete sequence (from START to end of DRINK) was 1.83 ± 0.39 s in freely reaching mice and 1.93 ± 0.35 s in restrained mice, and the duration of each phase was not statistically different between conditions (Table 1). Notably, the basic reach-to-grasp sequence was already observed at the earliest trials in naive mice (Figures S1A), suggesting a preexisting innate motor pattern for this behavior (Brácha et al., 1990). Taken together, the observed reach-to-grasp sequence for

Figure 1. Mice Rapidly Learn to Reach for Water Droplets, Performing Movement Sequences Similar to Pellet Reaching

(A and B) Schematics of freely moving (A) and head-fixed (B) mice in the water reaching task.

(C and D) Learning across ~30 min daily training sessions of (C) freely (n = 6) and (D) restrained (head-fixed, n = 6) reaching mice. Responded trials are the trials in which the mouse performed a reaching movement and touched the water spout target during the response period. They reflect the engagement of the mice with the task; it does not account for whether the reach was successful. Responded trials per hour reflect the rate of reaching movements that successfully targeted the water spout after droplet presentation. Water spout distance is the average distance across the session of the water spout to the tip of the snout. Mice attained plateau levels in the session marked with an asterisk ($p < 0.01$, RM ANOVA, Tukey post hoc test, compared with the first session and $p > 0.01$ compared to the last session). Black lines indicate mean ± SD; light lines indicate individual animals; error bars represent SD.

(E) Example of the reach-to-grasp sequence depicting the different phases of the movement in well-trained freely (left) and restrained (right) mice. The sequence of reaching for water droplets in freely and restrained mice resembles that of pellet reaching: lift the paw and aim the target (START), advance the forearm toward the target (ADVANCE), extend and open the fingers (OPEN), grasp the droplet (GRASP), supinate and retract the forepaw (RETRACT), bring the paw to the mouth and consume the reward (DRINK).

(F) The duration of each phase of the reaching sequence was measured in 30 trials per mouse, and a phase probability plot was created aligning the trials to the start of the grasping phase. Thick lines are the mean across mice (thin lines). Top, freely moving mice (n = 6); bottom, head-fixed mice (n = 6).

	Freely Reaching	Restrained Reaching
	n = 6	n = 6
START	116 ± 15	114 ± 29
ADVANCE	102 ± 23	93 ± 25
OPEN	26 ± 4	28 ± 6
GRASP	41 ± 6	54 ± 22
RETRACT	169 ± 26	141 ± 27
DRINK	1,373 ± 384	1,503 ± 360
Total	1,827 ± 388	1,933 ± 353

No statistically significant differences were found between the two conditions (two-way RM ANOVA, interaction p = 0.48, restraining factor p = 0.499).

liquid rewards closely resembles reaching behaviors previously described in mice, rats, and humans (Guo et al., 2015; Klein et al., 2012; Whishaw and Pellis, 1990).

Mice Can Reach in Multiple Directions Guided by Chemosensory Cues

A key element of the primate center-out paradigm is the directional reaching movements imposed by multiple target locations (Georgopoulos et al., 1982). Despite the similarity of reaching movements with primates, comparable directional reaching tasks in rodents have not been described so far. The anatomical differences among species (e.g., presence of ball-socket joint of the shoulder in primates) might preclude rodents from performing directional forelimb movements, allowing only the execution of a fixed and stereotyped reaching sequence.

We investigated this possibility by training head-fixed mice to perform directional reach-to-grasp movements to collect water droplets at three separate locations. Mice were trained to reach from a fixed starting point (resting bar) using the right forepaw. A motorized system displaced the water spout to different target locations around the snout of the mouse. Once the spout was moved to the target, mice had to hold the resting bar for 2 s in order to trigger the presentation of a ∼5 μL droplet of water. At the beginning of training, the water spout was located at nose tip level on the body midline. Across trials and on the basis of performance, the water spout was gradually moved away in one of three directions, 70° apart measured from the tip of the nose, until reaching the final target positions (Figure 2A). The final left, center, and right positions were spaced 4–6 mm from each other, and the target location was chosen pseudo-randomly from trial to trial. Mice rapidly learned to successfully reach for the three targets, and their performance plateaued after three days of training (Figure 2B). Interestingly, mice performed at similar levels for the three directions. Reaction times relative to reward presentation (i.e., release of the resting bar) were comparable for the three locations, suggesting that the detection ability of water reward presence is location independent within the studied space (Figure 2B).

To determine the extent of the "reaching space," we performed mapping experiments by moving the water spout into 46 positions radially disposed on an ellipsoidal grid (Figure 2C;

Experimental Procedures). The grid was composed of five concentric ellipses of increasing diameter (levels 1–5; Figure 2C; Experimental Procedures) centered at the nose tip (level 0). On average, mice consistently attained targets located within levels 0 and 2 (success rate > 80%). Reaching success dropped to 69.12 ± 10.84% at level 3 and below 40% at farther distances. Individual mice were also able to successfully reach to some targets in more distant levels (level 4) but often showing a bias toward the ipsi- or contralateral space (Figure S2C). These results underline that reaching ability of mice is more flexible than generally assumed (Whishaw et al., 2017) and further demonstrate that head-fixed mice are able to perform reward-oriented directional reaches to multiple locations.

To understand how mice detect and localize the spatial position of the water droplets, we performed a set of experiments during which different sensory modalities were removed or masked. For instance, rats orient the snout and actively sniff before initiating reach-to-grasp sequences in pellet reaching tasks (Whishaw and Tomie, 1989), while primates orient their gaze toward the target before initiating reaching movements (Biguer et al., 1982). In our experience, during the directional water reaching task, mice increased the rate of whisking and sniffing upon reward presentation, suggesting a role for whisker or olfactory systems.

When removing light or auditory cues, as expected (Hermer-Vazquez et al., 2007), there were no changes in the percentage of rewarded trials or reaction times to the reward presentation. It indicates that neither the reaching efficacy nor the detection of water drops depends on visual or auditory stimuli (Figures 2D and 2E). Remarkably, whisker trimming did not affect performance (Figures 2D and 2E), although the water spout was within whiskers' reach (Figure 2F) and despite the importance of the whisker system for locating and detecting objects in freely moving and head-fixed mice (Diamond et al., 2008; O'Connor et al., 2010). Finally, we tested the involvement of the olfactory system by directing the airflow away from the water spout using an air suction system. Surprisingly, we found a significant decrease in the number of rewarded trials (47.3 ± 28.1% compared with 82.16 ± 15.74% in control trials, paired t test p = 0.003; Figure 2D) accompanied by a significant delay in the reaction time (1.01 ± 0.35 s compared with 0.33 ± 0.1 s in control trials, paired t test p = 0.004; Figure 2E). These results were further confirmed by a pharmacologically induced lesion of the olfactory epithelium using methimazole (Brittebo, 1995), which has a transient behavioral effect in rats, with fast onset (12 hr) and slow recovery (more than 5 days post-injection; Genter et al., 1996). After initial training, mice received a vehicle injection and were tested on the following consecutive days (Figure S2D). At the end of the baseline period, mice were injected with methimazole and re-tested 18 hr later. Corroborating the air suction experiment, the number of rewarded trials dropped significantly (11.57 ± 15.78% compared with 81.95 ± 13.11% during baseline; p < 0.001, paired t test; Figure 2D), while the reaction time increased (2.37 ± 0.74 s compared with 0.37 ± 0.14 s in the control session, paired t test p = 0.003; Figure 2E). The effect of methimazole showed a recovery trend over the following sessions, which was transiently abolished by subsequent whisker trimming (Figure S2D), thus revealing a potential compensation by the somatosensory
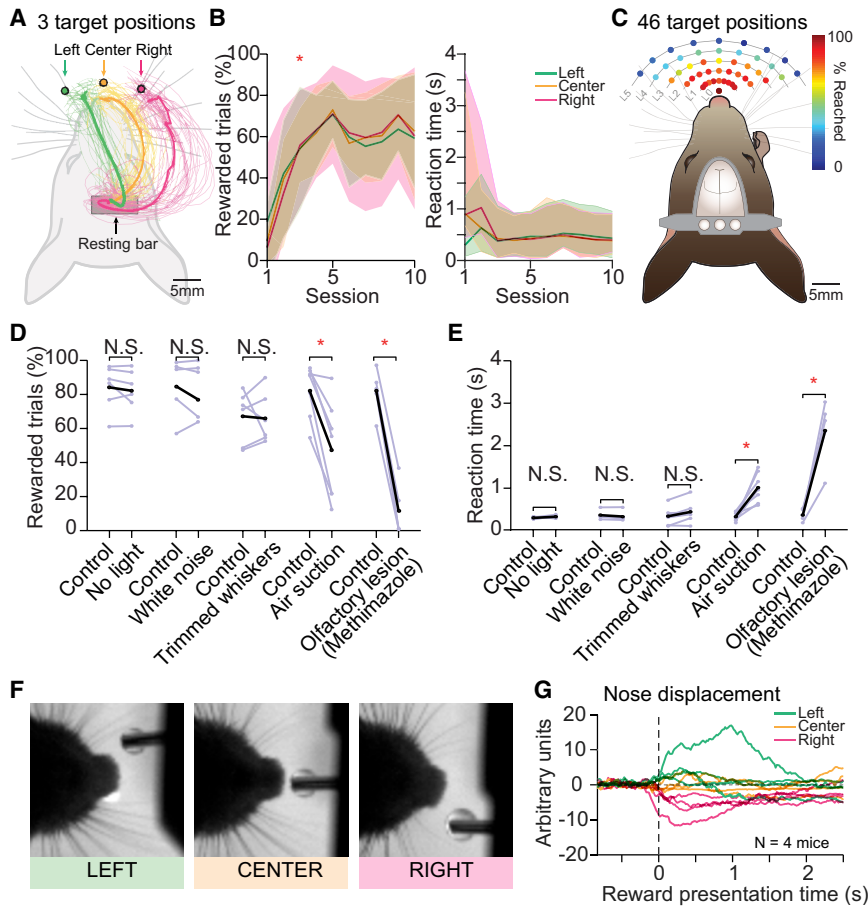
Figure 2. Head-Restrained Mice Can Reach for Water in Different Directions, Guided by the Olfactory System

(A) Top-view schematics of a head-fixed mouse trained to reach toward three different locations using a motorized system to automatically move the water spout in space (left, center, and right targets). Example reconstructions of the paw trajectories to each target during one session of a proficient mouse are depicted with thin colored traces, and the average trajectory is depicted with a thicker line.

(B) On the left, performance of directional reaching across training sessions (n = 19 mice). Trials are considered "rewarded" when the water droplet is retrieved from the water spout within 7 s from its presentation. Droplet retrieval was measured with an IR beam break detector. Mice attained plateau performance after three training sessions (*p < 0.01, Tukey post hoc test, compared with the first session and p > 0.01, RM ANOVA, compared with the last session). On the right, reaction time across sessions for the three directions tested. Reaction time was computed between the droplet presentation time and the first release of the resting bar.

(C) Map of the reaching space. Top-view schematics of a mouse reaching to 1 of 46 possible reward positions. The water presentation locations are disposed on a radial grid around the mouse snout spanning from level 0 (closest to the mouse) to level 5 (farthest from the mouse) (L0–L5). The color of each position represents the percentage of reached trials averaged across six mice (median). A trial was considered "reached" if the mouse touched the water spout within 10 s from water drop presentation.

(D and E) Perturbation of different sensory modalities in the three-directional reaching task shows that the chemosensory system is essential for the performance (rewarded trials, D) and detection (reaction time, E) of the water drops. The role of light ("No light," n = 6 mice; p = 0.37, paired t test for performance, and p = 0.16, Wilcoxon signed rank test for reaction time), sound ("White noise," n = 5 mice, p = 0.76 for performance and p = 0.05, paired t test for reaction time) and air perturbation ("Air suction," n = 7 mice, p < 0.01 for performance and p < 0.01, paired t test for reaction time) was tested on a trial-by-trial basis within session. The role of whiskers ("Whiskers trimming," n = 6 mice, p = 0.837 for performance and p = 0.04, paired t test for reaction time) and olfactory system ("olfactory lesion," n = 5 mice, p < 0.01 for performance and p < 0.01, paired t test for reaction time) was tested in separate sessions, before and after the treatment. Single mouse performance and timings are represented by light gray lines. Mean across mice in black. *p < 0.001.

(F) Top-view pictures of the snout of a representative mouse in the directional reaching task during water drop presentation in the left (green), center (yellow), and right (pink) position. Upon water delivery, mice direct the tip of the nose toward the reward.

(G) Snout tip video tracking (Experimental Procedures) showed that mice orient the snout toward the reward (n = 4 mice). Individual traces show the average nose displacement of each mouse for the three reward locations. The data are aligned to the time of reward presentation (dotted line).

system. Examination of video recordings during reward presentation suggested that mice actively located the reward by orienting the tip of their nose toward the target (Figures 2F and 2G; Movie S3). Taken together, these results suggest that chemosensation is used as the main modality to detect the presence and locate the position of the water droplets, raising the possibility of odor-based spatial maps under head fixation.

Reaching for Water Is Affected by Motor Cortex Inactivation

Motor cortex has been shown to play an important role in directional arm movements in primates (Georgopoulos et al., 1982; Graziano et al., 2002) and reaching for pellets in rats and mice

(Castro, 1972; Guo et al., 2015; Hira et al., 2015; Wang et al., 2017). Yet the execution of other forelimb behaviors, such as a timed lever task, does not seem to be affected by motor cortex lesions in rats, leading to the conclusion that skilled movements do not depend on motor cortex (Kawai et al., 2015). To study cortical involvement in the water reaching task, we performed cortical inactivation experiments.

First, we injected muscimol (a GABAa receptor agonist) into the motor cortex of mice that were proficient in the head-fixed reaching task. When tested under head fixation, mice did not initiate reaching movements (Figure S3A), supporting a role for motor cortex in goal-directed movement execution. To better control the timing, spatial extent and duration of cortical
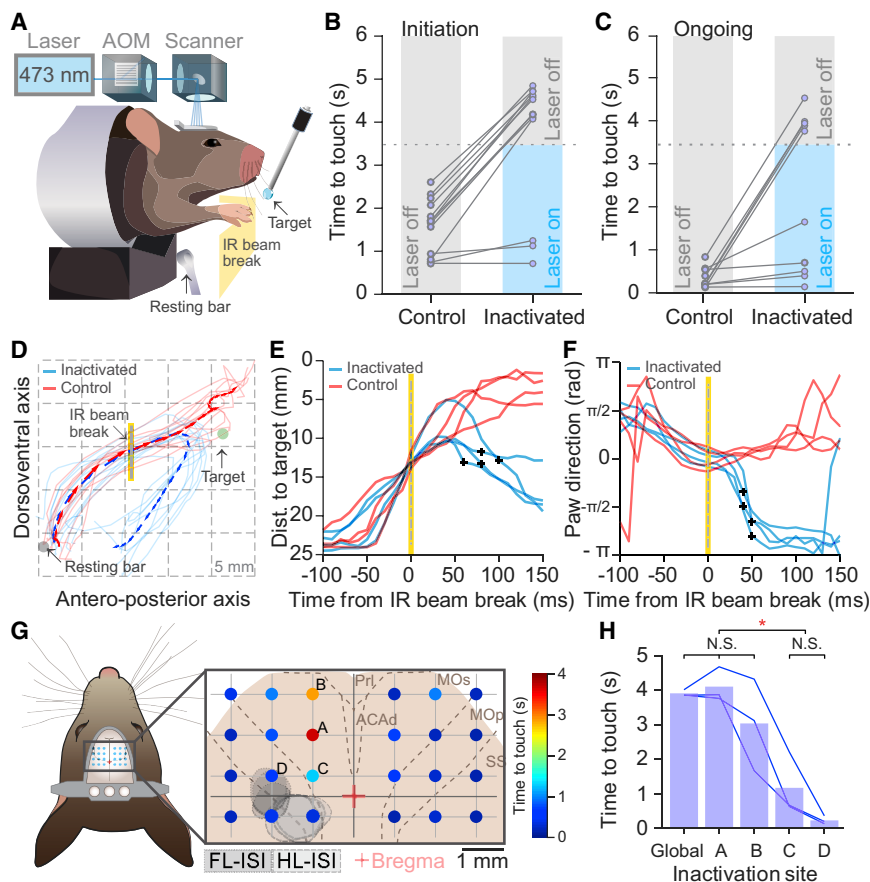
Figure 3. Initiation and Maintenance of Ongoing Reaching Movements Require Intact Motor Cortex Activity

(A) Side-view schematics of the automated optogenetic cortical inactivation system. Acousto-optically modulated (AOM) laser light (473 nm) was directed to illuminate frontal cortex (Experimental Procedures) using a galvanometric mirror system (scanner).

(B and C) Cortical inactivation was triggered either by the water reward presentation (movement initiation, B) or by crossing an IR beam sensor ("IR beam break," ongoing movement, C). Contralateral frontal cortex global inactivation delays the initiation (B, n = 13, p < 0.01, Wilcoxon signed rank test; laser power: 5 mW [n = 8] and 9 mW [n = 5]) and arrests ongoing execution (C, n = 10, p < 0.01, Wilcoxon signed rank test; laser power: 5 mW [n = 8] and 9 mW [n = 2]) of reaching movement. Data points represent the median time from inactivation onset to reward touch ("time to touch") for each mouse. Dotted gray lines indicate the end of laser illumination (3.5 s duration).

(D) Two-dimensional reconstruction (side view) of control (red) and inactivated (blue) reaching trajectories of a representative mouse (ten inactivated trials and ten control trials, thin traces) during a session of ongoing reaching inactivation. The mean trajectories are displayed with arrows reflecting the tangential direction of the movement.

(E and F) Deviation of inactivated movements from control trials following ongoing reaching inactivation (n = 4 mice). Individual traces are the mean values for each mouse (ten trials per condition). Black crosses indicate the time of statistical divergence (at the single mouse level) between inactivated (blue) and control (red) conditions of paw distance to the target (E, p < 0.001, Kolmogorov-Smirnov test) and tangential direction of the reaching trajectory (F, p < 0.001, Kuipers circular test).

(G) Spot inactivation map of the frontal cortex. On the left, schematics of a mouse top view showing the inactivation grid on top of the mouse skull. Insert on the right shows the 24-position inactivation grid; the color of each spot represents the time to touch the water spout (median across three mice) from IR beam crossing (inactivation onset, 3.5 s duration). Gray shades correspond to the intrinsic signal of forelimb (FL-ISI) and hindlimb (HL-ISI) of the same mice. Red cross, bregma; dotted lines, anatomical borders of the main cortical areas according to Allen Brain Atlas. Prl, prelimbic; ACAd, dorsal anterior cingulate area; MOp, primary motor; MOs, secondary motor; SS, primry somatosensory.

(H) Comparison between the time to touch under global frontal cortex inactivation and spots A, B, C, and D of the spot inactivation map. *p < 0.001, global versus D; p = 0.005, global versus C; p < 0.001, A versus D; p = 0.004, A versus C; p = 0.003, B versus D; p = 0.031, B versus C. Tukey post hoc tests, RM ANOVA. In (D)–(H), laser power is 5 mW.

inactivation, we silenced the motor cortex by optogenetic activation of GABAergic interneurons (VGAT-ChR2 mice) through a clear-skull cap preparation (Guo et al., 2014b). A scanning system was used to steer a laser beam (473 nm, 330 μm diameter; Figure 3A) to the frontal cortex (global motor cortex inactivation; Experimental Procedures). We found that optogenetic inactivation of the motor cortex at the time of reward presentation prevented the initiation of reach-to-grasp sequences (10 of 13 mice; p < 0.01, chi-square test; Figure 3B). Reaching proceeded at the offset of laser illumination (Figure S3B). This result is consistent with previous data (Guo et al., 2015) and confirms the involvement of motor cortex in the initiation of goal-directed movements. In a proportion of trials, however, mice were able to overcome the inactivation effect and collect the water reward while the laser illumination was on (16.07%, interquartile range 5.53%–26.92%, rewards collected during the inactivation period; Figure S3B).

Next, we silenced the motor cortex during the ongoing execution of reaching movements. An infrared beam positioned in the middle of the reaching trajectory was used to trigger the laser illumination when crossed by the paw of the mouse (Figure 3A). Mid-movement-triggered inactivation of the motor cortex diverted the arm trajectory downward impeding the mice from reaching the target until the end of the inactivation period (6 of 10 mice; p < 0.01, chi-square test; Figure 3C), when reaching was resumed (Figures 3C and S3C–S3G). During inactivation, however, mice were not paralyzed and were able to perform adjustment movements of the paw toward the resting bar and occasionally perform reaching movements while the laser illumination was on (18.96%, interquartile range 0%–44.83%, rewards collected during inactivation of ongoing reaches; Figure S3C; Movie S5). In a subset of mice (n = 4), we performed lateral-view video reconstructions of the reaching movements (Figures 3D and S3D–S3G) to study the kinematic effects of optogenetic inactivation.

We first measured the distance of the paw to the target during control and inactivated reaches (Guo et al., 2015). The distance to the target in inactivated trials differed from control trials after 82.5 ± 16.33 ms of laser illumination onset (p < 0.001, Kolmogorov-Smirnoff test; Figure 3E) confirming previous findings (Guo et al., 2015). However, visual inspection of reaching trajectories suggested a faster inactivation effect on forelimb movements. Indeed, we analyzed the tangential velocity of reaching trajectories (Della-Maggiore et al., 2004) and found that the direction of inactivated trajectories diverted from control trajectories 45.0 ± 5.77 ms after inactivation onset (p < 0.001, Watson-Williams test; Figure 3F). Taken together, these results suggest a faster communication channel between the cortex and the spinal cord than previously reported (Guo et al., 2015).

Finally, we performed a mapping experiment to determine the regional specificity of cortical inactivation effects during ongoing reaching movements. The laser beam was steered to 1 of 24 positions on the frontal cortex of both hemispheres (Figure 3G). As expected, inactivation spots on the right hemisphere (ipsilateral to the reaching paw) did not affect performance, while inactivation spots over the left motor cortex impaired reaching execution in the three mice tested (spots A and B, p < 0.001 and p = 0.003 compared with spot D, RM ANOVA Tukey post hoc test; Figures 3G and S3H). The strongest inactivation effect in spot A and B was comparable with that observed upon global inactivation (3.91 ± 0.07 and 4.1 ± 0.41 s "time to touch" for global and local inactivation, RM ANOVA Tukey post hoc test p = 0.204; Figure 3H) and was concentrated in a small cortical area within the secondary motor cortex (Allen Brain Atlas, 1.0 mm lateral to the midline and between 1.5 and 2.5 mm anterior to bregma). Taken together, these results show that, in our task, full activity of the motor cortex is necessary for the execution and maintenance of goal-directed reaching movements.

Directional Tuning in Motor Cortex Layer 2/3 Neurons
Next, we studied motor cortex involvement in the directional reaching task by optogenetically inactivating spot A or B (Figures 3G and S4A) before reaching initiation (Figure S4B) or during ongoing reaching (Figure S4C). On average, all three reaching directions were equally affected. These results can potentially be explained by two scenarios: either motor cortex is not involved in the directional coding, or all directions are equally represented in an intermingled fashion. In both cases, the single-spot inactivation would not result in directional effects. To discriminate between these two options, we performed two-photon calcium imaging of GCaMP6f expressing neurons in layer 2/3 (Figure 4A). We imaged 14 and 12 fields of view from spots A and B, respectively (n = 5 mice) and classified the neurons according to their activity. We observed task-related neurons showing peaks of fluorescence activity at different phases of the task, ranging from motor arrival to water spout touching. Consistent with the inactivation results, we found a large proportion of task-related neurons (spot A, 10.4 ± 5.3%; spot B, 4.2 ± 3.1%; Figure 4B) with a larger amount in spot A (24.5 ± 11.5 ROIs) than in spot B (8 ± 5.3 ROIs) (p < 0.002, Wilcoxon rank test).

To study directionality in the motor cortex, we focused on reach-related neurons (Experimental Procedures). Alignment of calcium traces to reach onset of left, center, and right trials (Figure 4C) revealed robust directionally selective responses of layer 2/3 neurons. Surprisingly, the majority of the neurons displayed strongly time-locked responses to only one reaching direction. A smaller proportion of the imaged ROIs displayed gradual responses to two or three directions, suggesting encoding of reaching directionality in the mouse motor cortex (Figures 4C and 4D). Within a given field of view, it was common to detect a similar number of reach-related neurons selective to the left, center, and right trials (Figure 4E), suggesting the absence of a reach-direction topographic map, which is consistent with the inactivation experiments (Figure S4).

Reaching for Water as a Handle for Instructed Motor Tasks
So far we have shown that head-fixed mice perform directional reach-to-grasp movements guided by the natural sensory information provided by the location of water drops. However, disentangling neuronal control of specific behavioral aspects such as motor execution, motor preparation, and sensory processing requires a controlled manipulation of sensory cues and timing of movement execution. We therefore explored the possibility of dissociating stimulus, motor action, and reward. Head-fixed mice were trained to perform reaching movements whose direction was arbitrarily instructed by a vibrotactile stimulus. Mice had to hold the resting bar for 2 s to initiate a trial and receive a sensory cue (60 or 200 Hz forepaw vibration) that instructed to which one of two fixed water spouts (left or right target) the mouse had to reach for in order to gain a water reward (Figures 5A and 5B). In addition, a variable delay period (ranging from 0.5 to 1.5 s) was instated between the vibrotactile cue and the motor execution (Figure 5A). During the delay period, mice were required to keep holding the resting bar and wait for a "go" cue before responding. Thus, unlike the chemosensory-guided experiments described before, goal-directed reaches were instructed by an arbitrary sensorimotor association learned through training, and rewards were delivered only after the correct motor output was performed.

After handling and shaping (Experimental Procedures; Figure S5A), mice were trained in the instrumental phase of the task, whose difficulty was gradually increased across sessions. As performance improved, the duration of the vibrotactile stimuli was shortened, and the onset of the go cue was delayed until reaching the final parameters of the task (Figure 5A). Two example raster plots aligned to the go cue (Figure 5C) depict the improvement in performance of a representative mouse. During the initial sessions, mice initiated relatively few trials (126.75 ± 34.48, session 1) with a low percentage of correct answers (50.01 ± 12.9%, session 1). In later sessions, the number of initiated trials was significantly higher (199.33 ± 67.17, session 15; one-tailed paired t test p = 0.011), as well as the proportion of correct answers (73.52 ± 14.4%, session 15; p < 0.001, one-tailed paired t test) (Figure 5D). To confirm that mice had learned the correct sensorimotor association, we assessed the discrimination ability (Experimental Procedures), which increased from 0.80 ± 0.70 in session 1 to 1.83 ± 0.82 in session 15 (p < 0.001, one-tailed paired t test; Figure 5E). Also, the number of gained rewards significantly increased over training (1.14 ± 0.51 rewards per minute in session 1 compared with 1.88 ± 0.65 in session 15, one-tailed paired t test p = 0.0023; Figure 5F).
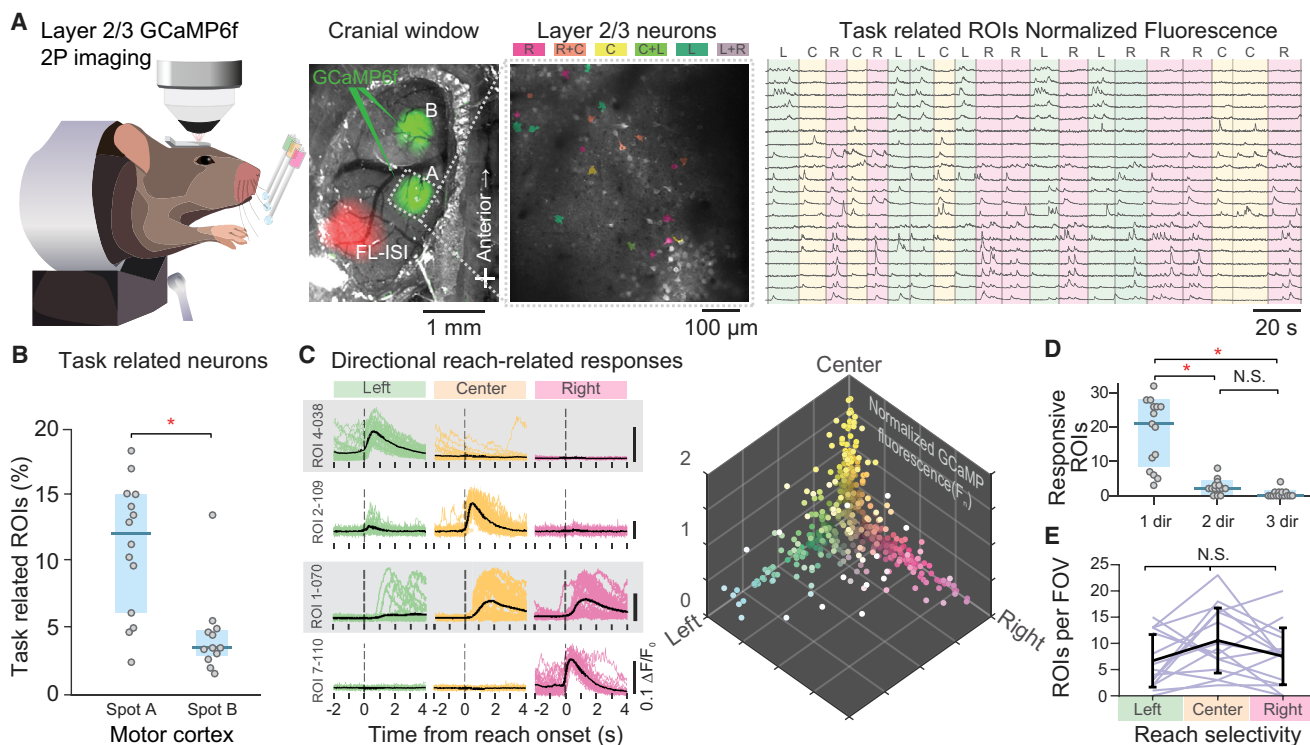
Figure 4. Two-Photon GCaMP6f Imaging of Motor Cortex Layer 2/3 Neurons Reveals Direction-Selective Activity in the Directional Reaching Task

(A) Left: side-view schematics of a head-fixed mouse under a two-photon microscope during the directional reaching task. Center: photomicrograph of the cranial window on top of the frontal cortex with AAV1-hSyn-GCaMP6f infected neurons (green fluorescence) in spots A and B. White cross, bregma; FL-ISI, forelimb intrinsic signal. Detailed field of view (FOV) of layer 2/3 neurons recorded during directional reaching task. Color-shaded ROIs correspond to task-related neurons and their trial type preference (color coding on the top: L, left; C, center; R, right). Right: normalized GCaMP6f fluorescence corresponding to the same ROIs; green, yellow, and pink shades correspond to the trial type (L, C, and R). Neurons were sorted according to their trial type preference.

(B) Percentage of task-related ROIs per FOV in spots A and B showing a higher proportion of related neurons in spot A. Light blue shades, 25th and 75th quartiles; horizontal line, median. *p = 0.004, Wilcoxon rank test.

(C) Calcium fluorescence traces ($\Delta F/F_0$) were triggered at the time of reaching onset for left, center, and right trials (time = 0). Left: four example ROIs showing different directional selectivity responses. Right: all reach-related ROIs projected in a three-dimensional space of normalized fluorescence response amplitude for left, center, and right trials. Each dot corresponds to one ROI with color-coded directional response.

(D) Number of ROIs per FOV with responses selective for one, two, or three directions showing that the majority of the imaged ROIs showed reach-related response to a single trial type. Light blue shades, 25th and 75th quartiles; horizontal line, median. *p < 0.05, Tukey post hoc test, Friedman RM ANOVA on ranks.

(E) Number of ROIs per FOV with direction selectivity preference to left, center, and right trials showing that, on average, all three direction-selective neurons are equally represented in each FOV. Black line represents the population mean; error bars represent SD.

In addition to learning the task structure and the arbitrary sensorimotor association, responses became more time locked across training. For instance, in correct trials of initial sessions, the time at which the reward was obtained was variable, while in later sessions, the time of the reward seemed more precisely locked to the go cue (Figure 5C). Confirming this observation, the variability of the reward timings decreased exponentially across sessions ($R^2 = 0.7830$, time constant 9.81 sessions; Figure 5G). The median reaction time, measured as the time between the onset of the go cue and the release of the resting bar, also decreased exponentially (asymptotically approaching 0.203 and 0.195 s for right and left trials respectively; Figures 5H and 5I) from 0.72 s (10%–90% interquantile range 0.27–2.31 s) during session 1 to 0.23 s (10%–90% interquantile range 0.14–0.89 s) at session 15 (Figures 5H, 5I, and S5B). Thus, these leaning curves suggest that mice achieve more precise motor control across training sessions.

Further training did not produce major improvements in performance (Figure S5C), showing that mice are able to rapidly (less than 20 sessions) learn a complex behavioral task with a set of rules including an arbitrary sensorimotor association, the ability of retaining a motor plan, and withholding motor execution until a go cue. Taken together, reaching for water in head-fixed mice is a promising paradigm with implications not only for motor, but also cognitive neuroscience research.

DISCUSSION

Directional Reaching, a Key Behavior in Modern Systems Neuroscience

The development of the center-out reaching task in primates has had an important impact by providing a framework for studying neuronal mechanisms involved in cortical coding of movements,
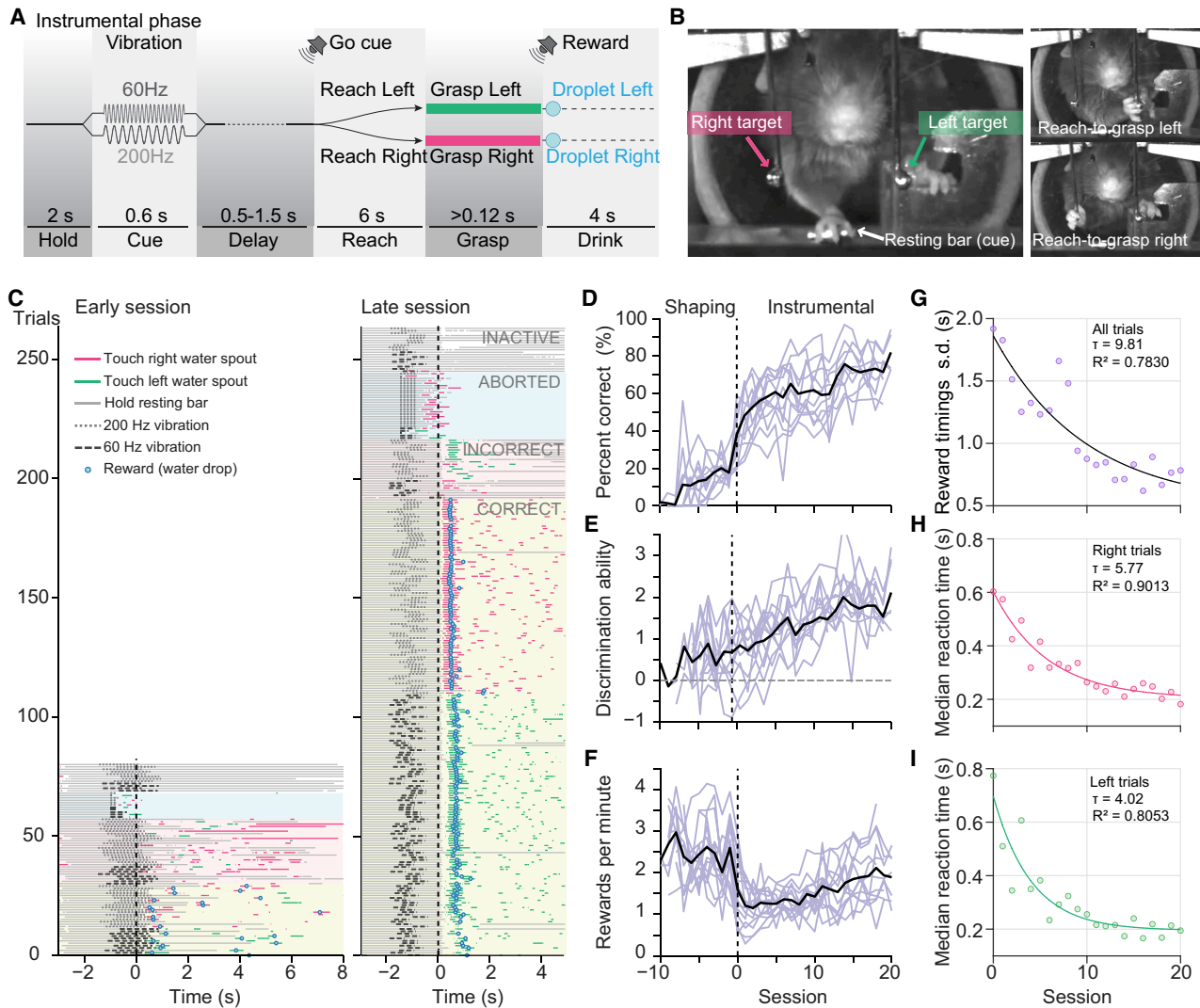
Figure 5. Directional Reaching Instructed by an Arbitrary Vibratory Cue Is Rapidly Learned

(A) Schematics of the task structure showing the sequence of events in a trial. Proficient mice were required to hold the resting bar for 2 s in order to receive a vibrotactile cue through the paw: a 200 Hz or 60 Hz sinusoidal vibration. The vibratory cue delivered by the resting bar was followed by a randomly variable delay period during which mice had to continuously hold the resting bar. The end of the delay period was signaled by a "beep" sound ("go" cue), upon which mice could release the resting bar and perform a reach-to-grasp movement toward the left or the right target. Correct responses with grasping of at least 120 ms were rewarded with a water drop delivered through the same water spout and signaled with a "click" sound. Incorrect responses (reaching for the incorrect target, not shown) were followed by a time-out period signaled with white noise (6–10 s). A new trial was started when mice returned the right paw to the resting bar and held it for 2 s.

(B) Pictures of a mouse performing the instructed directional reaching task. Vibrotactile stimuli (cues) were delivered through the resting bar. Two fixed water spouts located to the left or to the right of the animal were the targets for the reaches. The tip of the water spouts was enlarged with a small ball of solder in order to facilitate grasping.

(C) Example raster plots depicting the behavior of a mouse during early and late sessions of the instrumental phase of training. Trials are aligned to the "go" cue (0 s) and ordered according to the outcome of the trial (correct, incorrect, aborted, and inactive) and trial type (left or right) to ease visualization. The vibrotactile stimuli are represented with dashed lines. When the mouse is holding the resting bar or touching the water spouts, it is indicated with continuous colored lines (gray, pink, or green). Reward, if gained, is represented as a blue circle. Note the increase in performed trials and proportion of correct trials between the early and late session. Also, the timings of the behavior, such as the reaction time and the reward time, become more stereotyped. After receiving a reward, mice retract the paw to the mouth and drink the water. Note that after gaining and drinking the reward, mice typically perform subsequent reach-to-drink movements to collect the remaining water. This is visualized as water spout touches in the raster plot after reward delivery.

(D–I) Learning curves showing performance across sessions (n = 14 mice). (D) Percentage correct is the percentage of correct responses (direction of reaching) of all valid trials. (E) Discrimination ability of the vibrotactile stimulus. (F) Rewards per minute gained across sessions. (G) The variability within each session of the timing when mice received the water reward decreases exponentially across sessions. Plotted dots are the mean of 14 mice; solid line is the exponential fit. (H and I) Reaction times to the "go" cue measured as the release time of the resting bar decreases exponentially across sessions in left and right trials. Plotted dots are the median of 14 mice for right (H) and left (I) trials; solid lines, exponential fit.

sensorimotor transformations, and internal models (Georgopoulos et al., 1986; Scott and Kalaska, 1997; Shadmehr and Mussa-Ivaldi, 1994). Currently, comparable behavioral tasks for rodents are lacking, and the only paradigm approximating to directional reaching is the pasta matrix task (Ballermann et al., 2001). In this task, freely moving rats reach into an array of uncooked spaghetti pieces vertically displayed in an equally spaced grid. It was designed to determine the range and directionality of forelimb movements and as a sensitive method for assessing skilled movement in control and brain disease animal models (Ballermann et al., 2001). However, the fact that this is a task with no target replacement prevents its use for studying reaching behavior to the same location repeatedly during the session. Also, because rats are neither restrained nor forced to initiate the reaching movement from a specified starting point, the task might be solved through adjustments of the body position, losing the advantages of the well-controlled confinement settings of center-out tasks. Whether rats solving the pasta matrix task perform directional reaches is still unclear, to our knowledge. In the paradigm presented here, mice are required to reach for different targets using a motorized water spout or by setting up multiple independently controlled spouts. We found that head-fixed mice, similarly to primates, can perform directional reaches across an extensive space, thereby providing a promising behavioral framework for the dissection of the underlying neuronal mechanisms.

Advantages and Limitations of Reaching for Water

Reward-based training in rodents is typically performed under food or water restriction schemes. Water restriction is well tolerated by rodents and is widely used in head-fixed training (Guo et al., 2014a; Schwarz et al., 2010). Probably one of the most long-standing tasks under food restriction schemes is the pellet reaching task, which, however, yields very few trial repetitions. As a consequence, the amount of neuronal information and number of experimental manipulations that can be gathered per session is limited. A possible explanation for the small number of reported trials might be satiation. Typical pellet reaching tasks are constrained to commercial pellets of fixed weight (10–20 mg), which are relatively large compared to the daily food consumption of laboratory mice (4.4 ± 0.1 g; Bachmanov et al., 2002). In addition, pellet delivery must be performed either manually, which would be impractical for two-photon microscopy, or with sophisticated robotic apparatuses (Ellens et al., 2016; Guo et al., 2015). In contrast, water droplets can be delivered simply through a spout connected to a manual syringe or automatically with a gravity-based system gated by a water valve. Also, the size and value of the reward can be controlled by the experimenter according to task requirements. For instance, varying droplet sizes can be used to study value-based decision making or neuroeconomics. The palatability can be easily modified to make the reward more or less appetitive, and motivation can be manipulated by adding nutritional value (e.g., sweetened water, milk; Guo et al., 2014a). With a droplet size of 5 μL, it would be necessary to collect 1,160 rewards to attain the average daily consumption of water in laboratory mice of 5.8 ± 0.2 mL (Bachmanov et al., 2002). Indeed, using 5–10 μL drops in the different tasks presented here, the number

of trials per session in trained mice (typically more than 150) surpassed those reported in pellet tasks without reaching satiety (0.4–1.0 mL of water gained during training sessions). Also, water rewards offer the advantage of being rapidly consumed (1.5 ± 0.4 s in head-fixed mice; Table 1) without producing masticatory vibrations that could perturb the quality of electrophysiological or imaging recordings. Thus, reaching for liquid rewards is an alternative paradigm fulfilling many requirements of neurophysiological studies. Indeed, other forelimb-related tasks using water as reward have been recently described in combination with optogenetics, electrophysiology, or two-photon imaging. In these tasks, mice were trained to pull or push a joystick in a discrimination task (Morandell and Huber, 2017), reach and pull a joystick (Miri et al., 2017), touch a sensor upon a vibrotactile stimulus (Estebanez et al., 2017) or in a go/no-go task (Hasegawa et al., 2017). However, unlike the present paradigm, these tasks limit the behavioral repertoire to one or two motor outputs and are instructed only by arbitrary stimuli, and water rewards are delivered through licking of a water spout. The reaching for water paradigm is based on an ethologically relevant behavior (reach-to-grasp-to-mouth), which in its simplest form requires only three to five sessions of training. Also, it can be integrated in freely moving and head-fixed settings and adapted to different levels of complexity, according to experimental demands.

In our experience, overnight water deprivation was sufficient to motivate naive freely moving mice to engage in the water reaching task. Similarly, trained head-fixed mice also engaged rapidly in the task and showed learning curves and reach-to-grasp sequences akin to unrestrained mice. It has been recently reported that the elbow position during a pellet reaching task is different in head-fixed compared with freely moving mice and that different grasping strategies are used depending on task requirements, revealing a high degree of movement flexibility and motor adaptation (Whishaw et al., 2017). In the reaching for water task, head restrained mice performed more trials per session than freely reaching mice, performed fewer "in-vain" reaches and attained a plateau level of performance already by the third session, giving the impression that they are more "focused" on the task and learn faster than under freely moving conditions. With fewer exploration and grooming opportunities, head-fixed mice might concentrate more attentional resources on the task, possibly affecting learning and efficiency. Thus, motor strategies and neuronal control systems at play may not be the same under different restraining conditions.

An interesting observation was the initial interactions of freely moving mice with the water spout. After collecting the first rewards (fewer than five) through licking, all mice spontaneously responded with seemingly goal-directed reach-to-grasp movements aimed at the water spout during the first training session. This was even true when the water spout was at licking distance. Furthermore, the very first reaching sequence was much like those of later training sessions, highlighting the innate nature and possible ethological relevance of this behavior. However, this raises the question if reaching for water in its initial form can be considered a skill or whether task complexity or difficulty needs to be increased to study motor skill learning. Because the success rate rapidly dropped below 50% when the spout was positioned beyond a range of 5 mm (Figure 2C), increasing the

initial target position to a farther distance might be sufficient to reproduce some of the hallmarks of skill learning.

Another difference with the classical pellet reaching task is the scoring of the trial outcome. In pellet reaching, the reward is either brought to the mouth or not. In contrast, lost water droplets are harder to quantify because of water dispersion, evaporation, and the fact that water droplets, unlike solid objects, can be partially retrieved. These issues might be problematic in studies in which the emphasis is quantifying the success rate of reward consumption. Nevertheless, water reaching efficiency can also be estimated by the weight gained during the session and the total volume of water offered to the animal during the session. In addition, the number and timing of touches of the reward spout can be used to reliably measure performance and motor variability. As with pellet reaching, for more detailed analysis, offline video scoring or computer-vision solutions might need to be considered. Taken together, the directional reaching for liquid rewards is an alternative paradigm covering most aspects of the classic pellet reaching task adding the convenience and larger trial number of liquid-based rewards.

Olfactory Spatial Maps and Learning

Intriguingly, we found that mice use chemosensory cues and olfaction to detect and spatially localize the presence of water, suggesting the existence of odor-based spatial representation maps. This observation raises the question whether mice are able to detect water in air plumes through receptors similar to acid-sensing taste receptor cells (Zocchi et al., 2017) or they smell volatile impurities diluted in the water or the metallic waterspout itself. Freely moving rats are able to follow odor trails and localize odorants efficiently (Khan et al., 2012) on the basis of stereo olfaction provided by the comparison of left and right nostril odor information at the level of the olfactory bulb or the anterior olfactory nucleus (Kikuta et al., 2010; Rajan et al., 2006). Furthermore, the anterior pyriform cortex shows differential responses to ipsilateral and contralateral odor sources in rats, suggestive of spatial receptive fields (Wilson, 1997, 2001). Our data show that upon reward presentation, head-fixed mice sniffed and oriented the tip of the nose toward the target, suggesting an active sensing mechanism. Thus, olfactory information might be transformed into a spatial odor map by mechanisms similar to those involved in coding of auditory space (Konishi, 2003). After target localization, sensory information leads to a directional goal-directed reach. To achieve this, a possible underlying neuronal mechanism is the sensorimotor transformation similar to visual-motor transformations proposed for visually guided reaches in primates (Andersen et al., 1997). The question of whether such an olfactory-motor map exists and is learned during the task or is formed upon experience during development remains open.

Along these lines, what sensory modalities are used during the learning phase of the task is still unknown. Behavioral compensation by the whisker system after olfactory epithelium lesion suggests a possible re-learning mechanism for detecting the location and presence of the water droplet. Additional experiments with permanent lesion of the olfactory system or whisker-trimmed training might prove to be interesting models for studying re-learning and sensorimotor adaptation mechanisms.

Arbitrary Instructions for Directional Reaching

Inspired by other landmark primate paradigms used to study sensory discrimination and decision making (Hernández et al., 1997; Romo and Salinas, 2001), we have extended the olfactory-guided version of our directional reaching task and developed an instructed version on the basis of arbitrary sensorimotor associations. In the instructed version of the task, the sensory cue can be experimentally manipulated, enabling the discernment of neuronal computations for motor commands from those of sensory processing. Also, because the task imposes a delay period, solving the task requires a "memory" phase in which either the sensory cue or the motor plan to be performed are stored, allowing the study of working memory or motor planning and preparation. Importantly, because the delay period is variable, the task forces the mouse to attentively respond to an auditory go cue without relying on internal time counting. Taken together, the water reaching paradigm, with the natural-stimulus and arbitrary-stimulus (instructed) versions, shares many similarities with primate reaching tasks, whereby multiple motor outputs (reaching directions) could be used to study multiple choices in decision-making tasks and neuronal coding of different motor plans as well as sensory processing and stimulus discrimination.

Cortical Control of Reaching in Rodents

To what extent motor cortex is actually coding for motor function and how it contributes to movement control in primates and rodents is still under debate, and different conceptual frameworks have been put forward (Scott, 2008; Shenoy et al., 2013). Furthermore, there are also well-defined anatomical and functional differences in the organization of primate and rodent motor circuits (Lemon, 2008), raising the question of whether studying rodent forelimb behavior has translational value (Courtine et al., 2007). In rodents, cortical inactivation (Guo et al., 2015) and lesion experiments (Kawai et al., 2015) have led to seemingly contradictory conclusions, increasing the difficulty of interpreting the role of motor cortex in skilled movement execution. Using transgenic VGAT-ChR2 mice, we confirmed previous experiments by Guo et al. (2015) and observed a faster motor impairment effect after optogenetic inactivation (~45 ms) during ongoing reaching.

By performing a cortical inactivation mapping experiment (Guo et al., 2014b), we extended these results and revealed that inactivation effects were restricted to a small region in the secondary motor cortex (Allen Brain Atlas) of the contralateral hemisphere. Surprisingly, inactivation of primary motor cortex did not affect ongoing reaching movements. A possible interpretation is that after reaching initiation, the execution of the movement becomes independent of the primary motor cortex but still requires input from the secondary motor cortex (e.g., to maintain motor vigor). This would be consistent with recent data showing that the highest concentration of corticospinal "pre-grasping" neurons lies within the secondary motor cortex, while primary motor and somatosensory cortices are enriched with neurons displaying pre-reaching and post-grasping related activity (Wang et al., 2017). Intriguingly, the density of reach-related neurons is smaller in the primary motor cortex compared with the secondary motor cortex, suggesting that in order to obtain a behaviorally effect through optogenetic inactivation, a larger

cortical area might need to be silenced in the primary versus the secondary motor cortex.

Two-photon imaging of layer 2/3 neurons in this region (spots A and B; Figure 4) revealed, as well, a striking amount of task-related neurons. Although optogenetic inactivation in spots A and B produced similar behavioral effects, the proportion of reach-related neurons in spot A was ~2.5 times higher than those in spot B. This raises the question whether inactivation of spot B mediates an indirect behavioral effect through top-down connections onto spot A (Saiki et al., 2014) or whether inactivation in spot B affects task-related neurons located in other layers than layer 2/3. Similar to data from Wang et al. (2017), the onset of reach-related activity in layer 2/3 neurons takes place at different moments of the reach-to-grasp sequence (Figure 4C), ranging from ROIs with activity onset before movement initiation up to neurons with activity at the time of reward consumption. Further studies using electrophysiological recordings with a better time resolution than calcium imaging will allow resolving neuronal involvement in different phases of the task.

How the firing rate of individual neurons in the motor cortex is tuned to movement parameters can prove to be more challenging than understanding the processing of sensory information in the motor cortex (Harrison and Murphy, 2013). The confined settings of the center-out task in primates have permitted the necessary conditions for discovering directionally tuned neurons in the motor cortex during execution and preparation of reaching movements (Cisek and Kalaska, 2005; Georgopoulos et al., 1982). The directional reaching paradigm presented here has revealed the existence of highly selective, directionally tuned neurons in the mouse motor cortex. Interestingly, neurons selective for each of the three reaching directions were equally represented and intermingled within the same cortical area explaining why optogenetic inactivation did not produce a directionally biased effect (Figure S4). This is in stark contrast to another directional-motor task in which licking direction can be biased by specific manipulation of the ipsi- or contralateral hemisphere (Guo et al., 2014b), revealing possible distinct cortical mechanisms of motor control for licking and reaching and therefore highlighting the relevance of different behavioral paradigms for systems neuroscience.

Conclusion

A caveat of the use of rodents in neuroscience research is that translation to humans is more difficult than from primate research. In addition, the issue of whether neurological mechanisms between rodents and primates are homologous becomes harder to solve in the absence of comparable behavioral frameworks. Here, we have introduced an approach to a classical behavioral paradigm for mice that combines reach-to-grasp movements with water rewards yielding hundreds of trials per session. The reach-to-grasp sequence resembles that of pellet reaching, and importantly, head-fixed mice can reach for multiple directions, like primates. The instructed version of the reaching task breaks up the sensorimotor process into experimentally controllable components, allowing arbitrary sensorimotor mappings and, therefore, providing a powerful framework to study decision making and motor planning in mice. Furthermore, activ-

ity of cortical neurons is directionally selective, as expected from primate data. Taken together, this paradigm is akin to visually guided and center-out reaching tasks in primates, bridging the experimental gap between both animal models. It complements licking-based motor tasks in rodents by increasing the complexity of studied motor output, which is necessary to elucidate neural mechanisms of the motor system (Ölveczky, 2011). Remarkably, the reaching for water paradigm is flexible, rapidly engages mice, and facilitates investigation of a variety of topics, with the potential of exploiting genetic and state-of-the-art neuronal manipulation and recording tools available for mice (Luo et al., 2008).

EXPERIMENTAL PROCEDURES

Animals and Surgery

All experiments were approved by the Animal Care Committee of the University of Geneva and by the Direction générale de la santé of the Canton of Geneva. Mice were held under a controlled 12 hr light/dark cycle (7:00 lights on, 19:00 lights off) with *ad libitum* access to food and water until the start of behavioral experiments. Experiments were performed on adult (3–12 months old) mice, 31 male C57BL/6J wild-type mice and 26 VGAT-ChR2 (21 males and 5 females) (YFP-channelrhodopsin-2-expressing neurons under the control of the locus of the vesicular γ-aminobutyric acid [GABA] transporter, B6.Cg-Tg[Slc32a1-COP4*H134R/EYFP]8Gfng/J, obtained from Jackson Laboratory). Health status of all the animals was daily assessed as previously described (Guo et al., 2014a).

For head-fixed experiments, mice were subjected to head-bar surgery under standard aseptic procedures. All surgical procedures were conducted under isoflurane anesthesia (1.5%) in a custom-made apparatus equipped with a thermic plate heated at 37°C. Before surgery, nociceptive reflex responses (toe and tail pinch) were tested, and mice received analgesic and anti-inflammatory drugs (2.5 mg/kg intramuscular dexamethasone, 5 mg/kg subcutaneous [s.c.] carprofen, 0.1 mg/kg s.c. buprenorphine, 0.5 mL s.c. of 1% lidocaine under the scalp). The scalp was cleaned with ethanol (70%) and disinfected with a Betadine solution or chlorhexidine. Then, the scalp was excised and the remaining periosteum was removed with the aid of corneal scissors, sterile cotton swabs, and the blunt edge of a scalpel blade. Landmarks of interest, such as bregma and midline points, were marked with the scalpel and filled in with black ink (Edding permanent marker). The surface of the skull was gently scraped to increase adherence and covered with a thin layer of cyanoacrylate glue. A custom-made titanium head bar was placed on top of the interparietal bone and cemented to the skull with a layer of dental cement. The dental cement was spread over the skull up to the edge of the skin. After curating, dental cement was flattened with a dental drill and rendered translucent with cyanoacrylate (clear-skull cap preparation).

Cranial window surgical procedures for two-photon imaging were performed as previously described (Prsa et al., 2017) and following the same procedures as above. A craniotomy was performed over the left frontal cortex, and two virus injections (60 nL at 10 nL/min) were performed in the motor cortex through a beveled glass micropipette (20–30 μm outer diameter) with an oil hydraulic micromanipulator (Narishige). The virus (adeno-associated virus AAV1.Syn.GCaMP6f; UPENN) was diluted in 0.2% FastGreen in sterile saline to a final titer of 6.93×10^{12} genome copies/mL. Injection coordinates were chosen following optogenetic inactivation behavioral effects (see below): 1.5 mm and 2.5 mm anterior to bregma and 1 mm lateral to midline. Injections were performed at a depth of 300–350 μm from cortex surface. After virus injection, the pipette was slowly retracted, and the cortex was rinsed with saline and soaked for 1–2 min with dexamethasone (0.03%) before covering with a glass window. Hand-cut glass coverslips (150 mm thick) that matched the shape of the craniotomy were stuck together with optical adhesive (Norland 61) and curated with UV light for 1 min. The window was disinfected with ethanol (70%) and placed on top of the cortex, glued to the bone with cyanoacrylate glue, and secured with dental cement.

After surgery, mice were returned to their home cages and allowed to recover for at least 5 days. Daily supplemental doses of carprofen (2.5–5 mg/kg s.c.) were given if mice lost more than 1.5% of initial body weight.

Behavior

Before starting the behavioral training, *ad libitum* access to water was stopped. For head-fixed experiments, mice were handled daily and received ~1 mL of water per day until they reached ~80% of initial weight (typically 5–7 days after the start of water restriction). During the handling period, mice were habituated to the experimental setup, including habituation to the confinement tube (Guo et al., 2014a). The duration of head fixation was progressively increased at a rate of ~5 min/day. Behavior was controlled with a real-time Linux machine using MATLAB (MathWorks) routines based on Bcontrol (http://brodylab.princeton.edu/bcontrol). The real-time Linux system interfaced with different actuators such as water valves, motors, speakers, buzzers, and infrared sensors. Forelimb movements were detected using a transistor-based touch circuit (Slotnick, 2009) or an infrared beam break sensor (FX-301H Navi sensor and FT-A32 fiber optic; Panasonic) and acquired with an analog/digital PCI-6025e board (National Instruments). Infrared USB cameras (Firefly; Point Grey) were used to monitor the behavior of the animals. Images (376 × 240 pixels) were acquired at 60–100 frames/s using custom MATLAB routines. Mice were trained one session per day. Experiments were performed in the dark or under blue light-emitting diode (LED) illumination (Experimental Procedures, Motor Cortex Inactivation), unless stated otherwise.

Freely Moving Reaching for Water

C57BL/6J mice were water-deprived overnight before starting experiments and trained in a custom-made, transparent acrylic glass chamber (10 × 10 × 10 cm) with a vertical opening of 9.5 × 20 mm in the center of one of the walls (Figure 1A). The size of the slit allowed the mice to perform reaching movements with ease while limiting the protrusion of the snout up to the whisker pad. Outside the chamber, a vertical water spout (blunt 21G needle) in front of the center of the opening was used to deliver water droplets. The position was adjusted using a three-axis manual micromanipulator. During pilot experiments (data not shown) the spout was connected to a 1 mL syringe, and water droplets of ~10 μL were delivered manually. To better regulate the reward size, timing, and training parameters, 5 μL droplets were delivered through a calibrated gravity water system gated with a solenoid valve (The Lee Company) controlled by the real-time Linux system. On the first session of training, water-deprived mice were allowed to freely explore the chamber and received water droplets signaled by the "beep" sound of a buzzer (3.6 kHz, 80 ms). At the beginning of the first session, the water spout was located 10 mm away from the internal wall of the chamber ("start position," 0 mm). At this distance, when mice protruded their snout, the tip of the snout was close to the water spout, and naive mice were able to consume the water by licking. Upon the first water drop consumption, the water spout was progressively moved away, forcing the mice to switch from licking to reaching. This transition occurred spontaneously and usually started within the first five responded trials. Mice were free to use the preferred paw for reaching. According to performance, the water spout was moved away in steps of 0.5–1 mm. At every new session, the initial position of the water spout was set to the final position of the previous session. This procedure was continued until reaching a final distance of 7 ± 0.5 mm from the "start position" (typically achieved in the third session). Water spout touches were detected with a transistor touch circuit and used for classifying the outcome of the trials. If the water drop was not collected within 5 s (response period), the droplet was manually removed, and a new trial began after a 2 s timeout. At the beginning of each trial, a withholding period (3 s) was imposed, during which mice were required to not touch the water spout before the droplet delivery to discourage "in-vain" reaches. "In-vain" reaches refer to reaching movements directed to the water spout in the absence of a reward (Chen et al., 2014). If mice touched the water spout during this time, the withholding period was reinstated. Freely reaching mice were trained under white-light illumination. Following reports in pellet reaching tasks, session duration was set to ~30 min irrespective of whether mice were satiated or engaged in the task. If mice did not receive enough water, they received extra water to complement the daily dose of 1 mL/day.

To determine for how long and to what extent mice would perform the task, six months after the initial ten training sessions, mice were water deprived and re-trained for five sessions of 30 min. In the sixth session, mice were allowed to reach without time limitation. The criteria to end the session for each mouse was when two of these conditions were met: response rate dropped to about 50% (over the last 80 trials), mice did not perform a reaching movement for 12 consecutive trials (~2 min of inactivity), or mice performed three or more successful reaches without drinking the water reward.

Head-Fixed Reaching for Water

C57BL/6J mice underwent head-bar surgery and were trained to reach for water under head-fixed condition (Figure 1B). Handling and head restraining were performed as previously described, by taking care to minimize the discomfort of the animals (Guo et al., 2014a; Schwarz et al., 2010). Head-bars were fixed with an 8° angle to the sagittal plane for comfort. Elevated horizontal rods located 20–25 mm below the head-bar holders allowed the mice to rest their forepaws ("resting bar") while not behaving. Training was performed similarly to freely reaching mice. At the beginning of the first session, the water spout was disposed with an inclination of ~30° in a parasagittal plane (2–4 mm lateral to the midline) to emulate freely moving spatial configuration. The start position of the water spout was ~5 mm below the tip of the nose. At this position, mice were able to lick water droplets and touch the water spout if they groomed. Gentle stimulation of the whisker pad during the presentation of a water droplet promoted grooming and induced the transition to reaching. Whisker pad stimulation was performed with a blunt needle during the initial trials (< 20 trials) of the first session in five of six mice. The remaining mouse reached for the water drops spontaneously without necessity of whisker stimulation. Once mice started reaching, the distance of the water spout was gradually increased, as with freely moving mice, until a final distance of 5.5 ± 1 mm, which was typically achieved in the fourth session. Trial structure and session duration were the same as for freely reaching mice. Head-fixed mice were trained under white-light illumination.

Head-Fixed Directional Reaching

C57BL/6J with cranial windows and VGAT-ChR2 mice were trained under head fixation to reach for three different positions around the snout. The setup for these experiments was equipped with a motorized three-axis system (T-LSM100B; Zaber Tech) which allowed moving rapidly (25 mm/s) and precisely the water spout in space. Mice were trained to reach into three directions: left, center, and right. The center direction was aligned to the midline of the mouse, while the left and right directions held an angle of 70° with the midline from the start position. At the beginning of the first session the start position of the water spout was at the level of the tip of the nose in the horizontal plane 5 mm below the tip of the snout. During training, the water spout was pseudo-randomly presented to the mice in the three positions. Once the mice collected the reward two consecutive times at each position, the water spout was moved 0.25 mm away in each direction. This procedure was repeated until a final distance from the start position of 2.6 ± 1.25 mm for the central direction and 4.53 ± 1 mm for left and right directions. Mice were allowed to reach only with their right paw by blocking the left paw with a resting bar placed close to the shoulder (~15 mm below the head-bar holder, "paw blocker"). At the beginning of each trial, the water spout was advanced from the "home" position (40 mm away from the tip of the snout) to the target position (left, center, or right). A droplet of water (~5 μL) was made available only after mice continuously held for 2 s the "resting bar." Unlike the single-target reaching task, droplet delivery was not signaled with a "beep" sound, in order not to interfere with sensory modality experiments (see below). If the reward was not collected within 7 s (reaching period), the droplet was removed, the water spout retracted to the home position, and a new trial began. Droplet removal was detected with an infrared beam break sensor directed to the tip of the water spout (FX-301H Navi sensor and FT-AL05 fiber optic). Water spout touches and resting bar touches were detected with a touch circuit.

C57BL/6J mice pre-trained to reach for a single target location were used to study the extension of the "reaching space." In order to do so, the water spout was pseudo-randomly positioned in 1 of 46 locations around the mouse snout (Figure 2C). Target locations were arranged along nine directions on an ellipsoidal radial grid (major radius 7.5 mm, minor radius 12.5 mm), separated 17.5° from each other. On each direction, the spout could be presented at five equally spaced distances (Figure 2C), from the tip of the snout (level 0)

to the ellipsoidal grid perimeter (level 5). Each position was considered as "reached" if the mouse was able to touch the water spout within 10 s following the droplet presentation.

Head-Fixed Instructed Reaching

C57BL/6J head-fixed mice were trained in an instructed reaching task using directional reach-to-grasp movements as motor output and vibrotactile stimulation of the forepaw as instruction cues. The rig for this experiment was equipped with a resting bar for the right forepaw and a paw blocker for the left forepaw. The resting bar was a T-shaped bronze tube mechanically connected to a loudspeaker. Sinusoidal waves amplified by a subwoofer fed the loudspeaker, which transmitted low-frequency vibrations (≤200 Hz, below the hearing range of mice) to the resting bar for vibrotactile stimulation. Two static water spouts 14 mm apart (targets) were located at the anteroposterior level of the snout of head-fixed mice, one at each side of the mouse. The water spouts were 5–7 mm below the tip of the snout with an inclination of 25° in the sagittal plane. In this task, mice received vibrotactile stimulation (60 or 200 Hz) in the right forepaw followed by a variable delay period (0.5–1.5 s) and a "go" cue ("beep" sound). Upon the go cue, mice had to perform a reach-to-grasp movement to one of the two targets. After reaching and grasping a water spout for > 120 ms, correct reaches (60 Hz → left target, 200 Hz → right target) were rewarded with a water drop delivered through the same water spout. Incorrect reaches were punished with a timeout (6–10 s) and white noise. In order to initiate a new trial and receive a vibrotactile cue, mice had to hold the resting bar for 2 s ("hold" period). If the mice released the resting bar before the go cue, the trial was aborted.

To teach this task, training was divided into a "shaping" and an "instrumental" phase. Shaping started during the handling period, when mice were pre-trained to reach to the left and right water spouts by the delivery of water droplets during the corresponding vibrotactile cue (Figure S5A). At the beginning, mice detected, reached, grasped, and drank the water reward guided by the natural sensory information provided by the water droplet. After a few sessions (five to ten), mice started performing reach-to-grasp movements in anticipation to the water droplet delivery. When mice performed more than ~20% anticipated reaches, pre-training finished and the instrumental phase of training started. During the instrumental phase, mice would receive a water reward only after performing a reach-to-grasp movement toward the correct target. Along the instrumental phase training, the difficulty of the task was gradually increased. Initially, the duration of the vibration was set to 1.5 s, and the go cue was triggered while the vibratory stimulus was still ongoing. Thus, at this time of training, there was no delay period. To prevent slipping of the paw and facilitate the grasping behavior, the tip of the water spouts was enlarged with a drop of solder.

Water Detection: Sensory Modalities

In the directional reaching experiments, mice were able to precisely detect the correct location of the water spout and the moment of droplet delivery. We performed a series of experiments to determine the involvement of different sensory modalities. In these experiments, water drop delivery was not cued with any "beep" sound, thus the detection of the water reward was determined solely by the natural sensory information provided by the water delivery system.

Vision

The eventual role of visual cues in the task was tested by pseudo-randomly turning on and off, on a trial-by-trial basis, a 470 nm LED in the otherwise dark setup.

Audition

Auditory information (e.g., high-frequency noise produced by the motor-based water delivery system) was masked with white noise on a trial-by-trial basis. For this experiment, one mouse was excluded because during the control experiment the baseline performance was below 40%.

Somatosensation

To test the involvement of the whisker system, mice were anesthetized with isoflurane, and whiskers were trimmed with surgical scissors under a 10× magnification microscope. All whiskers from the left and right whisker pads were trimmed close to the base of the whisker. The day after trimming, mice were re-tested, and performance was compared with the pre-trimming session.

Olfactory System

For the purpose of this paper, we will refer to the olfactory system in a broad sense, including all possible chemosensory mechanisms (e.g., trigeminal chemosensory neurons in the olfactory epithelium). Mice are exquisitely sensitive to odors, and regular water contains volatile impurities that can be smelled. Also, the existence of taste receptor cells in mice that respond to water has been reported (Zocchi et al., 2017), raising the possibility that water could also be detected by smell. To study the involvement of the olfactory system, we performed two experiments: an air suction experiment aiming to remove odorants from the environment and a pharmacological lesion of the olfactory epithelium.

An air suction system was used to extract the odor from the experimental setup. The suction device was a 10 cm diameter flexible tube connected to an extraction hood placed in front of the mouse (behind the water spout), ~6 ± 2 cm away from the snout. The tube was gated with a shutter that, when open, extracted the air around the water spout away from the mouse. Within the same session, control and suction trials were intermingled by automatically opening and closing the shutter with a motorized system (T-LSM100B, Zaber Tech).

Methimazole is an antithyroid drug with olfactory toxic effects after intraperitoneal (i.p.) injection (Bergman et al., 2002). Trained mice received an i.p. dose of 50 μg/g body weight of methimazole (WXBC1539V; Sigma-Aldrich) dissolved in sterile saline. Baseline sessions after saline injection (three sessions) and methimazole injection (three sessions) were tested on consecutive days. Drug and saline injections were performed at the end of the light cycle (19:00), and mice were tested the day after at least 18 hr after the injection. Mice receiving methimazole were housed together and water deprived. In our experience, methimazole administration did not increase aggressive behavior of mice, and no injuries were observed.

To quantify the snout displacement following reward presentation, the top view of the mouse snout was recorded using a Firefly camera. Videos (100 frames/s) were automatically processed offline to estimate the snout position during the trials. The tip of the nose was divided into two square regions of interest (ROIs) covering the right and left halves of the snout tip (15 pixels lateral, 10 pixels anterior, and 30 pixels posterior) in a baseline image (before water drop presentation). For each frame, the mean intensity values of the left and right ROIs were normalized to baseline and subtracted to give the nose displacement value on a trial-by-trial basis.

Motor Cortex Inactivation

Pharmacological Inactivation: Muscimol

To test the involvement of motor cortex in reaching, C57BL/6J mice proficient in head-fixed reaching, were injected with Muscimol hydrobromide (Tocris) into the left motor cortex. Mice were anesthetized with isoflurane (1.5%) and received analgesic (except lidocaine) and anti-inflammatory drugs as described above. A small craniotomy (<1 mm diameter) was performed on the left skull without damaging the dura. Injection site was 1 mm lateral and 1.5 mm anterior to bregma. Muscimol injection was performed with a glass micropipette (Wiretrol II; P/N 5-000-2005; Drummond Scientific) beveled to obtain a sharp ~30 μm external diameter. A motorized micromanipulator (MP-285; Sutter Instrument) and an oil-hydraulic manipulator (MO-10; Narishige International) were used to control the position of the pipette and inject the drugs into the brain. The pipette was back-filled with mineral oil and tip-filled with either vehicle (0.9% NaCl, 0.1% Fast Green; experimental day 1, control session) or Muscimol dissolved in vehicle (5 mg/mL; experimental day 2, test session). The pipette was positioned at the center of the craniotomy and lowered to a vertical depth of 450 μm. A volume of 75 nL was injected at 15–20 nL/min, and the pipette was left in place for 5 min before retraction (O'Connor et al., 2010). The craniotomy was subsequently covered with Kwik Cast silicone (WPI) and secured with a thin layer of dental cement. At experimental day 2, the silicon layer was removed, and the drug injection was performed following the same protocol. Head-fixed reaching performance was assessed twice, 91 ± 18.93 min (Figure S3A, test 1) and 210.62 ± 19.54 min (Figure S3A, test 2) after the injection. Between sessions mice were left to recover in their home cage.

Optogenetic Inactivation: VGAT-ChR2

Optogenetic cortical inactivation was performed in VGAT-ChR2 head-fixed mice with clear-skull preparation (Guo et al., 2014b). For these experiments,

a 473 nm laser connected to a fiber port collimator (PAF-X-11-PC-A and PAF-X-5-A; Thorlabs) and a galvanometric scanning mirror system ("scanner") was used to steer blue modulated light to the motor cortex, thanks to an acousto-optical modulator (AOM) and a shutter (OBIS 473 LX; Coherent) controlled in real time by the Linux behavioral system. The laser beam diameter at the skull level was 330 μm (D4σ) (Spiricon beam profiler). In all of the experiments, the calibrated laser power was set to 5 or 9 mW. To prevent visual confounds, a blue LED (470 nm) was lit at the beginning of each trial to mask the light of the laser. During the inter-trial interval, the LED mask was turned off.

We performed two types of experiments: global and single-spot inactivation. For global inactivation, the laser beam was steered over the left hemisphere to form an ellipsoidal shape (major axis 2.1, minor axis 1), centered at 1.3 mm lateral and 1.8 mm anterior to bregma, with a 24° clockwise rotation angle (as seen from the top with the nose pointing to 12 o'clock). The illumination pattern cycled at 40 Hz and passed through forelimb-related motor cortical areas, such as the rostral forelimb area (0.9 mm anterior, 2.7 mm lateral to bregma) and caudal forelimb area (1.8 mm anterior, 0.8 mm lateral to bregma; Hira et al., 2015; Zingg et al., 2014). Within a session, ~50% of the trials were pseudo-randomly chosen for inactivation (no more than three consecutive inactivated trials).

To construct a cortical inactivation-map, we performed single-spot inactivation experiments steering the laser to a single spot within an equally spaced grid (1 mm separation) of 12 targets on each hemisphere. The grid extended from 0.5 mm posterior to bregma and 1 mm lateral to the midline until 2.5 mm anterior to bregma and 3 mm lateral to the midline. Optogenetic illumination took place in 80% of the trials, and the inactivation target was chosen pseudo-randomly (avoiding the same spot in consecutive attempts) and alternating left and right hemispheres. Photo-stimulus temporal profile was sinusoidally modulated (40 Hz) and linearly attenuated during the final 100 ms of the stimulation to prevent excitation rebound (Guo et al., 2014b).

We studied cortex involvement in two aspects of reaching: the initiation and the maintenance of the reaching movement. Each aspect was studied in separate sessions. For the initiation experiments, the laser beam was turned on simultaneously with the delivery of the water drop (i.e., before reaching was initiated). After the end of the photostimulation, mice still disposed of 3.5 s to perform the reaching movement and collect the water drop before the trial ended. For the maintenance experiments, photostimulation started after a reaching movement had already been initiated. Reaching movements were detected online when an infrared (IR) beam (FX-301H Navi sensor and FT-A32 fiber optic, Panasonic) was broken by the reaching movement. The IR system was located between the resting bar and the water spout (Figure 3A), such that the IR beam was broken only with reaching movements and not with other kind of movements, such as paw adjustments. In all cases, the duration of the optogenetic illumination was 3.5 s per trial.

Two-Photon and Intrinsic Imaging

To study the activity of motor cortex layer 2/3 neurons during the directional reaching paradigm, well-trained mice expressing GCaMP6f were imaged in a custom built two-photon microscope (MIMMS; https://openwiki.janelia.org/wiki/display/public/Home) controlled by Scanimage 5 (https://vidriotechnologies.com). A 16× 0.8 NA objective (Nikon) with a pulsed laser excitation wavelength at 920 nm (Ultra II, tunable Ti:Sapphire laser; Coherent) and a resonant scanner system (Thorlabs) were used to image GCaMP6f fluorescence changes in a 650-by-650 μm field of view (FOV) at 29.38 frames/s. Laser power was modulated with a pockel cell (350-80-LA-02, Conoptics) to a maximum of 10 mW. Images were continuously acquired using a gated photo multiplier tube (H11706P-40 SEL; Hamamatsu) and digitally written in 16-bit format to disk in separate files triggered by the behavioral system using a TTL pulse. For statistical purposes, imaging sessions typically lasted for 90–150 consecutive trials (30–50 repetitions per reaching direction), and up to two different FOVs were imaged during the same behavioral session. Virus injection settings typically yielded confined infection foci of ~600 μm diameter when observed under the two-photon microscope. To avoid re-sampling the same neurons, the imaging field was located using stereotactic coordinates at different depths (ranging from 150 to 300 μm below the surface) and manually adjusted using reference images of previous sessions.

To obtain anatomical functional references, the cortical representation of the right forelimb and hindlimb were determined through intrinsic signal imaging

(ISI). At the end of the experimental period, mice were subject to ISI as previously described (Prsa et al., 2017). Briefly, isoflurane anesthetized mice received a 1 s vibrotactile stimulation of the forelimb or hindlimb while the surface of the skull or the cranial window was illuminated with a collimated red LED light (630 nm) and imaged at 10 fps with 256-by-332 pixel resolution using 12-bit camera (QImaging). Stimulation and image acquisition were controlled with Ephus (http://scanimage.vidriotechnologies.com/display/ephus/Ephus). Twenty post-stimulus frames were averaged and subtracted to baseline average image (1.5 s before stimulus). Ten to 20 repetitions were averaged, spatially filtered, and smoothed with a 5-by-5 pixel Gaussian low-pass filter. Intrinsic signal was manually threshold (>50% of the maximal signal; Ayling et al., 2009) and overlaid to a cortex or skull picture.

Two-Photon Image Analysis

Two-photon images were registered to a template (session average) in order to correct motion artifacts using a two-dimensional discrete Fourier transform and cross-correlation approach. The cross-correlation between single frames and the template was computed by multiplying the two-dimensional discrete Fourier transform of one with the complex conjugate of the Fourier transform of the other and taking the inverse Fourier transform of the product. The row and column location of the peak cross-correlation was taken as the vertical and horizontal displacement of the frame to the template respectively. Next, registered images were semi-automatically processed using published algorithms (Pnevmatikakis et al., 2016) to automatically detect ROIs and extract GCaMP fluorescence traces across time. Extraction parameters were empirically determined by iterations of extraction and visual curation of ROIs and calcium traces. $\Delta F/F_0$ was computed by using the algorithm $[F(t) - F_0]/ F_0$, where $F(t)$ is the fluorescence intensity at each time point and F_0 is the mean fluorescence of the full calcium trace. For comparing among different ROIs, calcium traces were normalized (F_n) using the algorithm $F(t)/[F_0 + 3 \times F_{std}]$, where F_{std} is the SD of the full calcium trace.

Reaching Trajectory Analysis

To perform a top-view reconstruction of the paw trajectory during the reaching movements, two Firefly cameras were used to simultaneously record the frontal and lateral view of head restrained mice. Videos (100 frames/s) were acquired and processed offline to manually track the position of the forepaw during reaching movements using custom MATLAB routines.

Data and Statistical Analysis

Data were analyzed using custom-written MATLAB routines. Population average values are the mean ± SD unless stated otherwise. Statistical tests were performed using MATLAB or SigmaPlot (Systat Software). Repeated-measures (RM) ANOVA and Student's t tests were applied when data distribution fulfilled parametric assumptions. In the following cases data were transformed to perform parametric tests: "in-vain" reaches per trial (Figure S1C) and mean duration of reaching phases (Figure S1D) were log-transformed. The post hoc test of choice was the Tukey post hoc test, unless stated otherwise. To determine if individual mice were behaviorally affected by optogenetic inactivation, a chi-square test was performed comparing the proportion of reached trials during and after the inactivation period in inactivated versus control trials.

Discrimination ability (d) in the instructed reaching task was computed as follows: $d = z$ (correct left response rate) + z (correct right response rate), where z is the inverse of the normal cumulative distribution, and the correct response rate is the number of correct responses divided by the total number of responses to the left or right targets. A rate of 70% correct responses to both targets corresponds to $d = 1.05$ (Morandell and Huber, 2017).

To determine if the activity of an ROI was task related, calcium traces were aligned to a given behavioral event (trial start, drop delivery, reaching onset, and water spout touch) in order to obtain behaviorally triggered calcium traces (typically 30–50 per reaching direction per FOV). The normalized fluorescence signal was compared using a paired t test using the average fluorescence intensity in a time window of 1 s before and 1 s after the triggering event. An ROI was considered to be related to the behavioral event when the p value was below 0.0001 and the magnitude of the effect was >0.2 (Chen et al., 2013). Because of the relatively long time window used for the statistical analysis, the onset of task-related GCaMP fluorescence could take place after the

triggering event. Thus, the classification of reach-related ROI does not necessarily imply that the activity of the neuron is involved in controlling reaching but might be related to grasping (Wang et al., 2017), arm retraction, or even reward consumption.

SUPPLEMENTAL INFORMATION

Supplemental Information includes five figures and five movies and can be found with this article online at https://doi.org/10.1016/j.celrep.2018.02.042.

AUTHOR CONTRIBUTIONS

Conceptualization, C.B., G.L.G., and D.H.; Software, C.B. and G.L.G.; Formal Analysis, C.B. and G.L.G.; Investigation, C.B. and G.L.G.; Writing – Original Draft, G.L.G.; Writing – Review & Editing, C.B., G.L.G., and D.H.; Visualization, G.L.G.; Supervision, G.L.G. and D.H.; Funding Acquisition, G.L.G. and D.H.

DECLARATION OF INTERESTS

The authors declare no competing interests.

REFERENCES

Andersen, R.A., Snyder, L.H., Bradley, D.C., and Xing, J. (1997). Multimodal representation of space in the posterior parietal cortex and its use in planning movements. Annu. Rev. Neurosci. 20, 303–330.

Ayling, O.G.S., Harrison, T.C., Boyd, J.D., Goroshkov, A., and Murphy, T.H. (2009). Automated light-based mapping of motor cortex by photoactivation of channelrhodopsin-2 transgenic mice. Nat. Methods 6, 219–224.

Bachmanov, A.A., Reed, D.R., Beauchamp, G.K., and Tordoff, M.G. (2002). Food intake, water intake, and drinking spout side preference of 28 mouse strains. Behav. Genet. 32, 435–443.

Ballermann, M., Metz, G.A., McKenna, J.E., Klassen, F., and Whishaw, I.Q. (2001). The pasta matrix reaching task: a simple test for measuring skilled reaching distance, direction, and dexterity in rats. J. Neurosci. Methods 106, 39–45.

Bergman, U., Ostergren, A., Gustafson, A.L., and Brittebo, B. (2002). Differential effects of olfactory toxicants on olfactory regeneration. Arch. Toxicol. 76, 104–112.

Biguer, B., Jeannerod, M., and Prablanc, C. (1982). The coordination of eye, head, and arm movements during reaching at a single visual target. Exp. Brain Res. 46, 301–304.

Brácha, V., Zhuravin, I.A., and Bures, J. (1990). The reaching reaction in the rat: a part of the digging pattern? Behav. Brain Res. 36, 53–64.

Brittebo, E.B. (1995). Metabolism-dependent toxicity of methimazole in the olfactory nasal mucosa. Pharmacol. Toxicol. 76, 76–79.

Castro, A.J. (1972). The effects of cortical ablations on digital usage in the rat. Brain Res. 37, 173–185.

Chen, T.-W.W., Wardill, T.J., Sun, Y., Pulver, S.R., Renninger, S.L., Baohan, A., Schreiter, E.R., Kerr, R.A., Orger, M.B., Jayaraman, V., et al. (2013). Ultrasensitive fluorescent proteins for imaging neuronal activity. Nature 499, 295–300.

Chen, C.-C.C., Gilmore, A., and Zuo, Y. (2014). Study motor skill learning by single-pellet reaching tasks in mice. J. Vis. Exp. (85)

Cisek, P., and Kalaska, J.F. (2004). Neural correlates of mental rehearsal in dorsal premotor cortex. Nature 431, 993–996.

Cisek, P., and Kalaska, J.F. (2005). Neural correlates of reaching decisions in dorsal premotor cortex: specification of multiple direction choices and final selection of action. Neuron 45, 801–814.

Courtine, G., Bunge, M.B., Fawcett, J.W., Grossman, R.G., Kaas, J.H., Lemon, R., Maier, I., Martin, J., Nudo, R.J., Ramon-Cueto, A., et al. (2007). Can experiments in nonhuman primates expedite the translation of treatments for spinal cord injury in humans? Nat. Med. 13, 561–566.

Della-Maggiore, V., Malfait, N., Ostry, D.J., and Paus, T. (2004). Stimulation of the posterior parietal cortex interferes with arm trajectory adjustments during the learning of new dynamics. J. Neurosci. 24, 9971–9976.

Diamond, M.E., von Heimendahl, M., Knutsen, P.M., Kleinfeld, D., and Ahissar, E. (2008). 'Where' and 'what' in the whisker sensorimotor system. Nat. Rev. Neurosci. 9, 601–612.

Ellens, D.J., Gaidica, M., Toader, A., Peng, S., Shue, S., John, T., Bova, A., and Leventhal, D.K. (2016). An automated rat single pellet reaching system with high-speed video capture. J. Neurosci. Methods 271, 119–127.

Esposito, M.S., Capelli, P., and Arber, S. (2014). Brainstem nucleus MdV mediates skilled forelimb motor tasks. Nature 508, 351–356.

Estebanez, L., Hoffmann, D., Voigt, B.C., and Poulet, J.F.A. (2017). Parvalbumin-expressing GABAergic neurons in primary motor cortex signal reaching. Cell Rep. 20, 308–318.

Genter, M.B., Owens, D.M., Carlone, H.B., and Crofton, K.M. (1996). Characterization of olfactory deficits in the rat following administration of 2,6-dichlorobenzonitrile (dichlobenil), 3,3′-iminodipropionitrile, or methimazole. Fundam. Appl. Toxicol. 29, 71–77.

Georgopoulos, A.P., Kalaska, J.F., Caminiti, R., and Massey, J.T. (1982). On the relations between the direction of two-dimensional arm movements and cell discharge in primate motor cortex. J. Neurosci. 2, 1527–1537.

Georgopoulos, A.P., Schwartz, A.B., and Kettner, R.E. (1986). Neuronal population coding of movement direction. Science 233, 1416–1419.

Graziano, M.S., Taylor, C.S., and Moore, T. (2002). Complex movements evoked by microstimulation of precentral cortex. Neuron 34, 841–851.

Guo, Z.V., Hires, S.A., Li, N., O'Connor, D.H., Komiyama, T., Ophir, E., Huber, D., Bonardi, C., Morandell, K., Gutnisky, D., et al. (2014a). Procedures for behavioral experiments in head-fixed mice. PLoS ONE 9, e88678.

Guo, Z.V., Li, N., Huber, D., Ophir, E., Gutnisky, D., Ting, J.T., Feng, G., and Svoboda, K. (2014b). Flow of cortical activity underlying a tactile decision in mice. Neuron 81, 179–194.

Guo, J.-Z., Graves, A.R., Guo, W.W., Zheng, J., Lee, A., Rodríguez-González, J., Li, N., Macklin, J.J., Phillips, J.W., Mensh, B.D., et al. (2015). Cortex commands the performance of skilled movement. eLife 4, e10774.

Harms, K.J., Rioult-Pedotti, M.S., Carter, D.R., and Dunaevsky, A. (2008). Transient spine expansion and learning-induced plasticity in layer 1 primary motor cortex. J. Neurosci. 28, 5686–5690.

Harrison, T.C., and Murphy, T.H. (2013). Towards a circuit mechanism for movement tuning in motor cortex. Front. Neural Circuits 6, 127.

Hasegawa, M., Majima, K., Itokazu, T., Maki, T., Albrecht, U.-R., Castner, N., Izumo, M., Sohya, K., Sato, T.K., Kamitani, Y., and Sato, T.R. (2017). Selective suppression of local circuits during movement preparation in the mouse motor cortex. Cell Rep. 18, 2676–2686.

Hermer-Vazquez, L., Hermer-Vazquez, R., and Chapin, J.K. (2007). The reach-to-grasp-food task for rats: a rare case of modularity in animal behavior? Behav. Brain Res. 177, 322–328.

Hernández, A., Salinas, E., García, R., and Romo, R. (1997). Discrimination in the sense of flutter: new psychophysical measurements in monkeys. J. Neurosci. *17*, 6391–6400.

Hira, R., Ohkubo, F., Ozawa, K., Isomura, Y., Kitamura, K., Kano, M., Kasai, H., and Matsuzaki, M. (2013). Spatiotemporal dynamics of functional clusters of neurons in the mouse motor cortex during a voluntary movement. J. Neurosci. *33*, 1377–1390.

Hira, R., Terada, S., Kondo, M., and Matsuzaki, M. (2015). Distinct functional modules for discrete and rhythmic forelimb movements in the mouse motor cortex. J. Neurosci. *35*, 13311–13322.

Kawai, R., Markman, T., Poddar, R., Ko, R., Fantana, A.L., Dhawale, A.K., Kampff, A.R., and Ölveczky, B.P. (2015). Motor cortex is required for learning but not for executing a motor skill. Neuron *86*, 800–812.

Khan, A.G., Sarangi, M., and Bhalla, U.S. (2012). Rats track odour trails accurately using a multi-layered strategy with near-optimal sampling. Nat. Commun. *3*, 703.

Kikuta, S., Sato, K., Kashiwadani, H., Tsunoda, K., Yamasoba, T., and Mori, K. (2010). From the Cover: Neurons in the anterior olfactory nucleus pars externa detect right or left localization of odor sources. Proc. Natl. Acad. Sci. U S A *107*, 12363–12368.

Kleim, J.A., Hogg, T.M., VandenBerg, P.M., Cooper, N.R., Bruneau, R., and Remple, M. (2004). Cortical synaptogenesis and motor map reorganization occur during late, but not early, phase of motor skill learning. J. Neurosci. *24*, 628–633.

Klein, A., Sacrey, L.-A.R., Whishaw, I.Q., and Dunnett, S.B. (2012). The use of rodent skilled reaching as a translational model for investigating brain damage and disease. Neurosci. Biobehav. Rev. *36*, 1030–1042.

Konishi, M. (2003). Coding of auditory space. Annu. Rev. Neurosci. *26*, 31–55.

Lemon, R.N. (2008). Descending pathways in motor control. Annu. Rev. Neurosci. *31*, 195–218.

Luo, L., Callaway, E.M., and Svoboda, K. (2008). Genetic dissection of neural circuits. Neuron *57*, 634–660.

Miri, A., Warriner, C.L., Seely, J.S., Elsayed, G.F., Cunningham, J.P., Churchland, M.M., and Jessell, T.M. (2017). Behaviorally selective engagement of short-latency effector pathways by motor cortex. Neuron *95*, 683–696.e11.

Morandell, K., and Huber, D. (2017). The role of forelimb motor cortex areas in goal directed action in mice. Sci. Rep. *7*, 15759.

O'Connor, D.H., Huber, D., and Svoboda, K. (2009). Reverse engineering the mouse brain. Nature *461*, 923–929.

O'Connor, D.H., Clack, N.G., Huber, D., Komiyama, T., Myers, E.W., and Svoboda, K. (2010). Vibrissa-based object localization in head-fixed mice. J. Neurosci. *30*, 1947–1967.

Ölveczky, B.P. (2011). Motoring ahead with rodents. Curr. Opin. Neurobiol. *21*, 571–578.

Peters, A.J., Chen, S.X., and Komiyama, T. (2014). Emergence of reproducible spatiotemporal activity during motor learning. Nature *510*, 263–267.

Pnevmatikakis, E.A., Soudry, D., Gao, Y., Machado, T.A., Merel, J., Pfau, D., Reardon, T., Mu, Y., Lacefield, C., Yang, W., et al. (2016). Simultaneous denoising, deconvolution, and demixing of calcium imaging data. Neuron *89*, 285–299.

Prsa, M., Galiñanes, G.L., and Huber, D. (2017). Rapid integration of artificial sensory feedback during operant conditioning of motor cortex neurons. Neuron *93*, 929–939.e6.

Rajan, R., Clement, J.P., and Bhalla, U.S. (2006). Rats smell in stereo. Science *311*, 666–670.

Romo, R., and Salinas, E. (2001). Touch and go: decision-making mechanisms in somatosensation. Annu. Rev. Neurosci. *24*, 107–137.

Sacrey, L.-A.R., Alaverdashvili, M., and Whishaw, I.Q. (2009). Similar hand shaping in reaching-for-food (skilled reaching) in rats and humans provides evidence of homology in release, collection, and manipulation movements. Behav. Brain Res. *204*, 153–161.

Saiki, A., Kimura, R., Samura, T., Fujiwara-Tsukamoto, Y., Sakai, Y., and Isomura, Y. (2014). Different modulation of common motor information in rat primary and secondary motor cortices. PLoS ONE *9*, e98662.

Sasaki, K., Ono, T., Nishino, H., Fukuda, M., and Muramoto, K.I. (1983). A method for long-term artifact-free recording of single unit activity in freely moving, eating and drinking animals. J. Neurosci. Methods *7*, 43–47.

Schwartz, A.B., Kettner, R.E., and Georgopoulos, A.P. (1988). Primate motor cortex and free arm movements to visual targets in three-dimensional space. I. Relations between single cell discharge and direction of movement. J. Neurosci. *8*, 2913–2927.

Schwarz, C., Hentschke, H., Butovas, S., Haiss, F., Stüttgen, M.C., Gerdjikov, T.V., Bergner, C.G., and Waiblinger, C. (2010). The head-fixed behaving rat—procedures and pitfalls. Somatosens. Mot. Res. *27*, 131–148.

Scott, S.H. (2008). Inconvenient truths about neural processing in primary motor cortex. J. Physiol. *586*, 1217–1224.

Scott, S.H., and Kalaska, J.F. (1997). Reaching movements with similar hand paths but different arm orientations. I. Activity of individual cells in motor cortex. J. Neurophysiol. *77*, 826–852.

Shadmehr, R., and Mussa-Ivaldi, F.A. (1994). Adaptive representation of dynamics during learning of a motor task. J. Neurosci. *14*, 3208–3224.

Shenoy, K.V., Sahani, M., and Churchland, M.M. (2013). Cortical control of arm movements: a dynamical systems perspective. Annu. Rev. Neurosci. *36*, 337–359.

Slotnick, B. (2009). A simple 2-transistor touch or lick detector circuit. J. Exp. Anal. Behav. *91*, 253–255.

Taylor, D.M., Tillery, S.I., and Schwartz, A.B. (2002). Direct cortical control of 3D neuroprosthetic devices. Science *296*, 1829–1832.

Wang, X., Liu, Y., Li, X., Zhang, Z., Yang, H., Zhang, Y., Williams, P.R., Alwahab, N.S.A., Kapur, K., Yu, B., et al. (2017). Deconstruction of corticospinal circuits for goal-directed motor skills. Cell *171*, 440–455.e14.

Whishaw, I.Q., and Pellis, S.M. (1990). The structure of skilled forelimb reaching in the rat: a proximally driven movement with a single distal rotatory component. Behav. Brain Res. *41*, 49–59.

Whishaw, I.Q., and Tomie, J.A. (1989). Olfaction directs skilled forelimb reaching in the rat. Behav. Brain Res. *32*, 11–21.

Whishaw, I.Q., Pellis, S.M., and Gorny, B.P. (1992). Skilled reaching in rats and humans: evidence for parallel development or homology. Behav. Brain Res. *47*, 59–70.

Whishaw, I.Q., Faraji, J., Kuntz, J., Mirza Agha, B., Patel, M., Metz, G.A.S., and Mohajerani, M.H. (2017). Organization of the reach and grasp in head-fixed vs freely-moving mice provides support for multiple motor channel theory of neocortical organization. Exp. Brain Res. *235*, 1919–1932.

Wilson, D.A. (1997). Binaral interactions in the rat piriform cortex. J. Neurophysiol. *78*, 160–169.

Wilson, D.A. (2001). Receptive fields in the rat piriform cortex. Chem. Senses *26*, 577–584.

Wong, C.C., Ramanathan, D.S., Gulati, T., Won, S.J., and Ganguly, K. (2015). An automated behavioral box to assess forelimb function in rats. J. Neurosci. Methods *246*, 30–37.

Xu, T., Yu, X., Perlik, A.J., Tobin, W.F., Zweig, J.A., Tennant, K., Jones, T., and Zuo, Y. (2009). Rapid formation and selective stabilization of synapses for enduring motor memories. Nature *462*, 915–919.

Zingg, B., Hintiryan, H., Gou, L., Song, M.Y., Bay, M., Bienkowski, M.S., Foster, N.N., Yamashita, S., Bowman, I., Toga, A.W., and Dong, H.W. (2014). Neural networks of the mouse neocortex. Cell *156*, 1096–1111.

Zocchi, D., Wennemuth, G., and Oka, Y. (2017). The cellular mechanism for water detection in the mammalian taste system. Nat. Neurosci. *20*, 927–933.
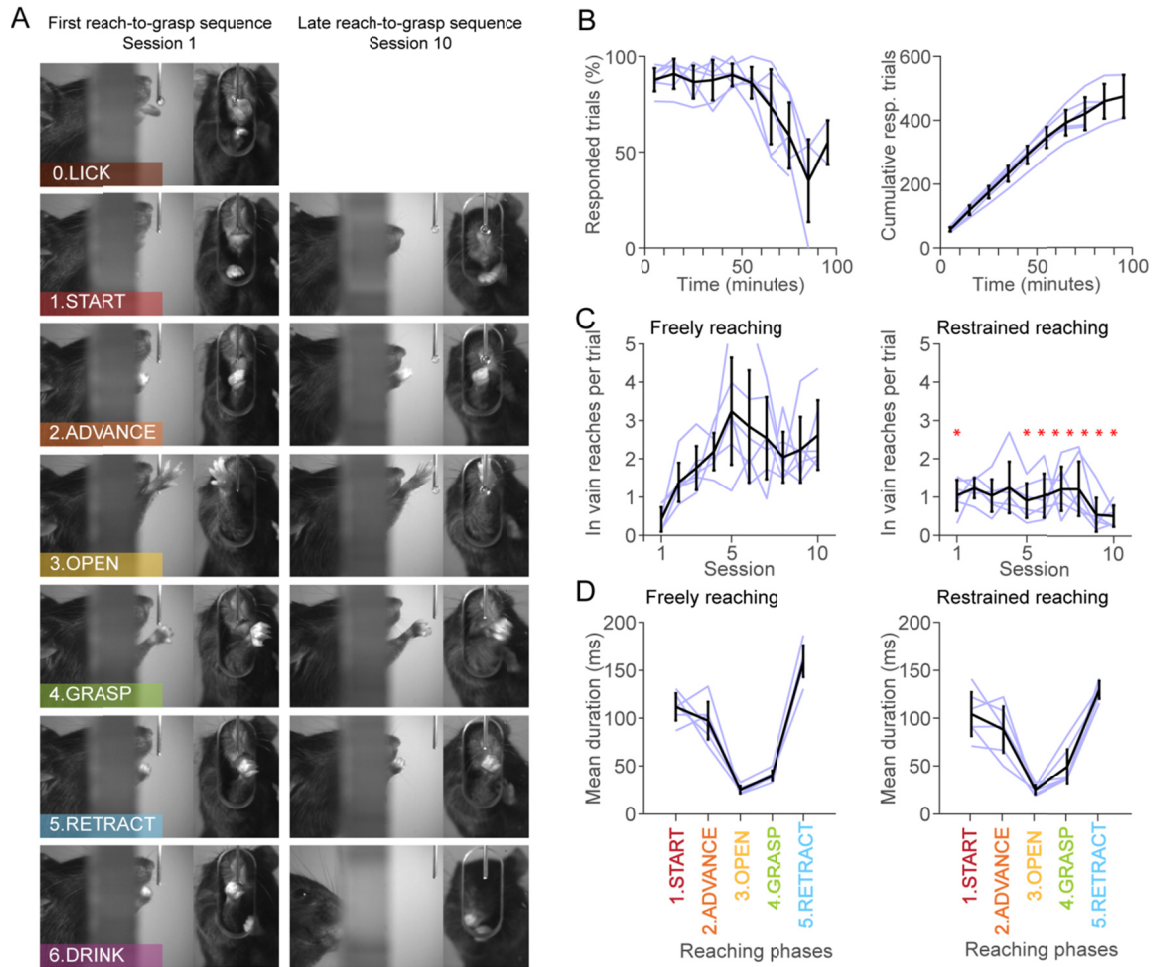
Supplemental Information

Directional Reaching for Water

as a Cortex-Dependent

Behavioral Framework for Mice

Gregorio Luis Galiñanes, Claudia Bonardi, and Daniel Huber

Figure S1. Reaching for water characterization. Related to Figure 1. (A) Example of the first reach-to-grasp sequence (left column) performed by a freely moving mouse after consuming the water through licking (LICK) which resembles the sequence of the same mouse after extensive training (session 10, right column). Note the position of the water spout in session 1 was closer to the box than in session 10. (B) Proficient mice were tested in a freely reaching session without time restriction (see Methods) to evaluate the engagement in the task and the maximal number of reaches performed. On the left, percentage of responded trials shows that mice were engaged in reaching for at least 60 minutes. On the right, the cumulative number of responded trials shows that mice performed a total of 438 ± 60 trials. Data binned in 10 minute intervals (C) Freely moving mice tend to perform more "in-vain" reaches (see Methods) per trial than head-fixed mice in later sessions (* $p < 0.01$ Tukey post hoc test after significant session per treatment interaction RM ANOVA). (A-C) Black lines mean $\pm$ s.d.; light lines individual animals. (D) Mean duration of the different phases of the reach-to-grasp sequence are comparable between freely moving and head-fixed mice (see table 1). (B-D) Black lines are the mean $\pm$ s.d.; thin lines individual animals.
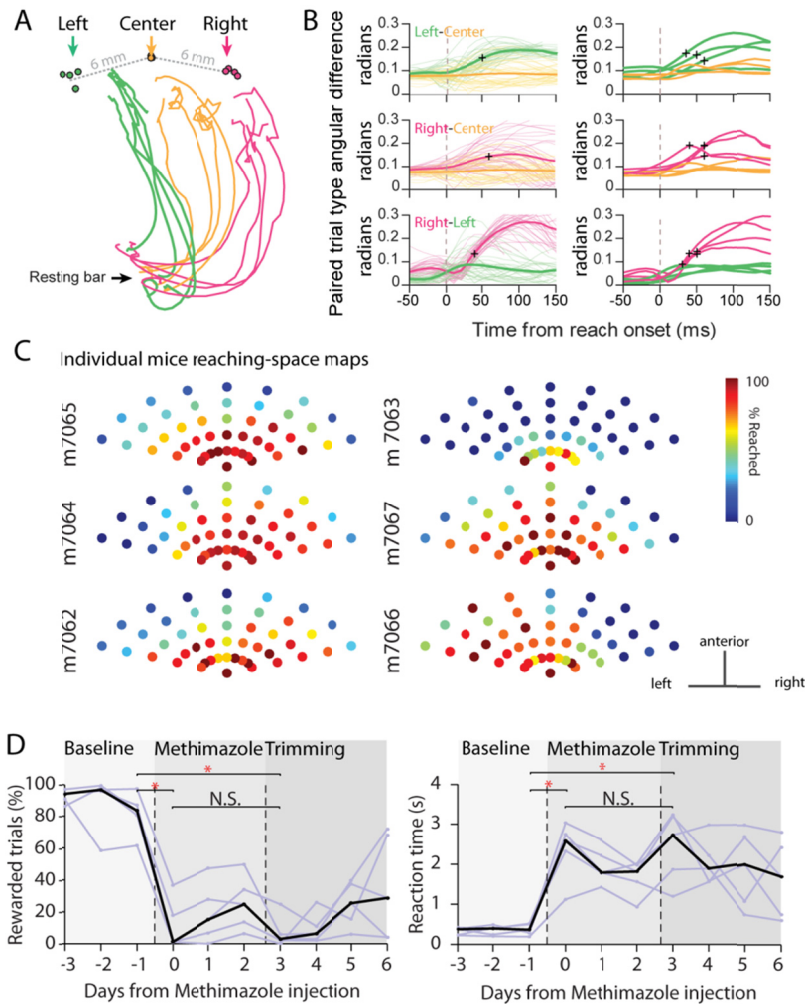
Figure S2. Multiple-target reaching and sensory guidance characterization. Related to Figure 2. (A) Top view of average reaching trajectories for N = 4 mice to the left, center and right targets. (B) Pair-wise angular difference between two trial types. Top: Left trials against the average of central trials (left-central, green) and central trials against the average of central trials (central-central, yellow). Middle: Right-central (magenta) and central-central (yellow). Bottom: Right-left (magenta) and left-left (green). Black crosses indicate statistically significant (p < 0.001, Kuipers circular test) differences between the angular differences of the corresponding trial types compared. Left column: one session for one example animal; thin traces individual trials, thick traces average. Right column: data from 4 mice (average angular difference within a session). Mean divergence time: 49.1 ± 10 ms from reaching onset. (C) Individual reaching space maps. (D) Performance (left) and reaction time (right) across consecutive sessions to study the effect of pharmacological lesion (methimazole i.p. injection) of the olfactory epithelium (N=5 mice). After methimazole injection performance significantly dropped and reaction times increased. Subsequent testing showed a recovery trend (although statistically not significant) which was subsequently abolished by whisker trimming. * *p* <0.001 (rewarded trials) and * *p* = 0.002 (reaction times), Tukey post hoc test, RM ANOVA. Black lines median across animals; light lines individual animals.
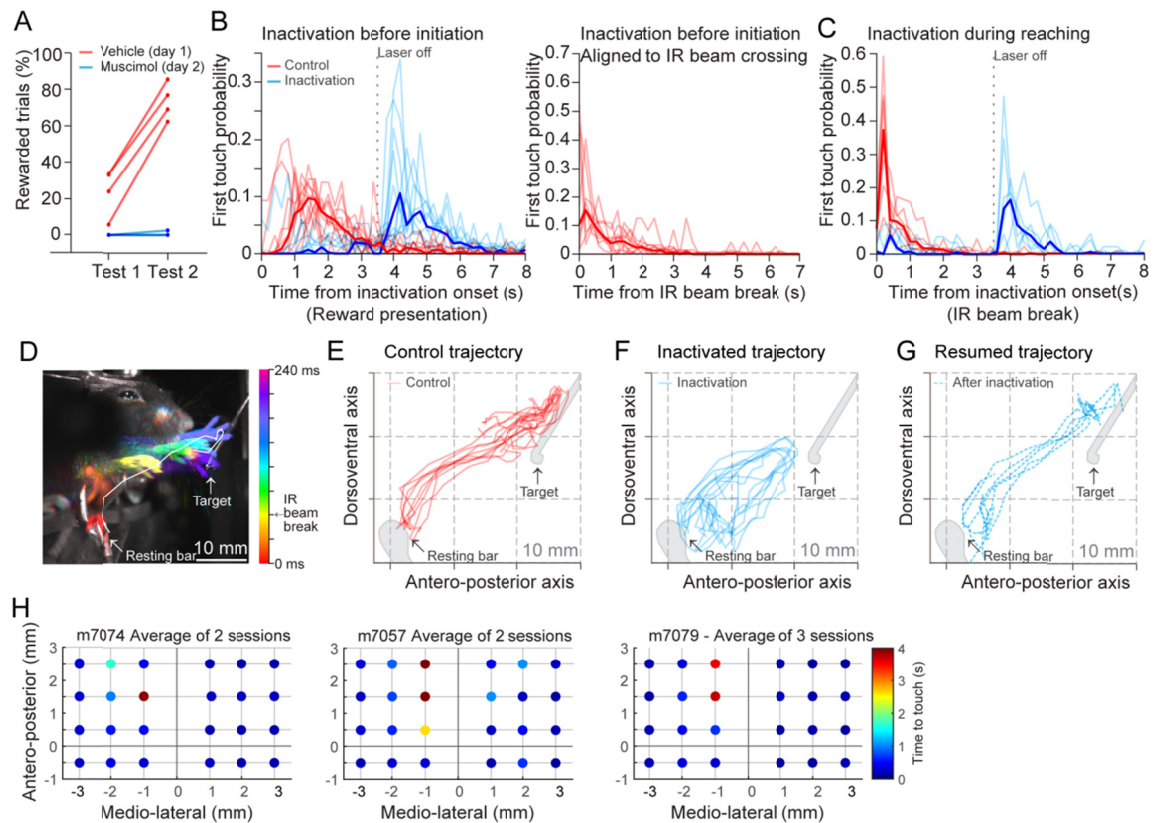
Figure S3. Cortical inactivation characterization. Related to figure 3. (A) 75 nl muscimol (5 mg/ml) injection in the motor cortex precludes mice from performing goal directed reaches under head-fixation. (B) On the left, touch probability of the water spout as a function of time for control (red) and inactivated trials (blue). Laser illumination was turned on simultaneously with water drop presentation (i.e. inactivation before initiation of reaching). During inactivated trials, affected mice (N = 10) initiated reaching after laser illumination was turned off. However, some mice occasionally overcame the optogenetic inactivation effect and managed to perform reaching movements and touch the water spout during the inactivation period. Right panel, the same data as on the left panel for control trials aligned to IR beam break for comparison with control data in C. (C) Touch probability plot for inactivation experiments during ongoing reaching. In inactivated trials, laser illumination was turned on at the time of IR beam crossing. Affected mice (N = 6) reached the water spout after the end of laser illumination. In some trials, mice overcame the inactivation effect and reached the target while laser illumination was on. (D) Lateral view colored projection of selected frames of video recorded data highlighting the position of the paw during the reaching trajectory of a control trial. Time references in the color bar on the right. The manually reconstructed trajectory is overlaid in white. (E-F) Reconstructed reaching trajectories of a representative mouse under control (E) and inactivated (F-G) trials. Trajectories in G correspond to the reaching movements performed at the end of the inactivation period of inactivated trials. (H) Individual inactivation maps.
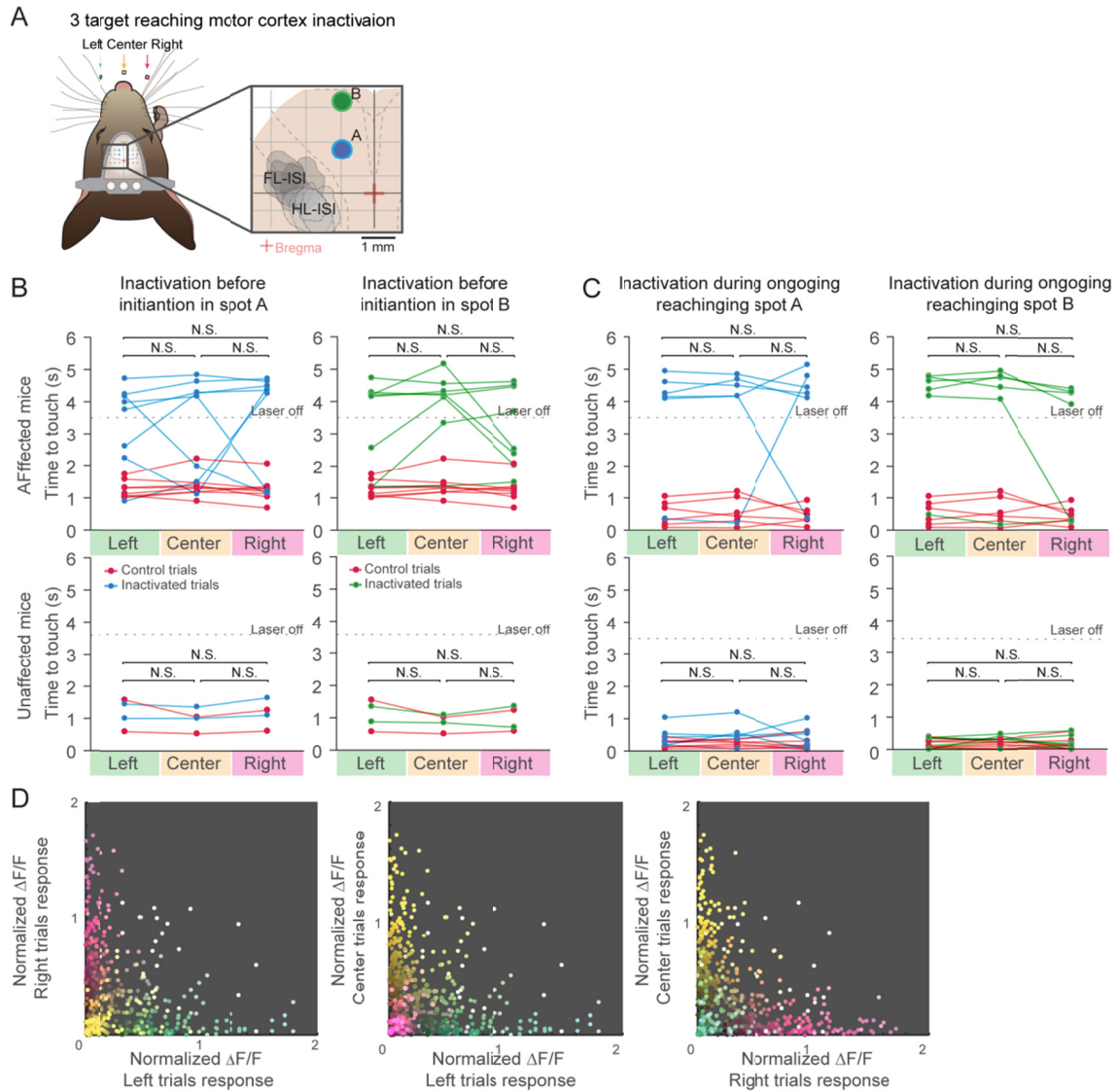
Figure S4. Involvement of secondary motor cortex in directional reaching. Related to figure 4. (A) Schematics of spot A and spot B optogenetic inactivation during the directional reaching task. Red cross: bregma; dotted lines: borders of main cortical regions according to Allen Brain Atlas. Gray shades correspond to the intrinsic signal of forelimb (FL-ISI) and hindlimb (HL-ISI) of the same mice used in the inactivation experiments. (B) Optogenetic inactivation before reaching initiation in spot A (left column) or B (right column) produced similar behavioral effects irrespective of trial type (left, center or right) in mice affected by optogenetic inactivation (top row). On average, unaffected mice did not show higher probability of being affected for any of the trial types (bottom row). (C) Same as (B) but inactivation during ongoing inactivation. (D) Same data as Figure 4C projected into a 2 dimensional space.
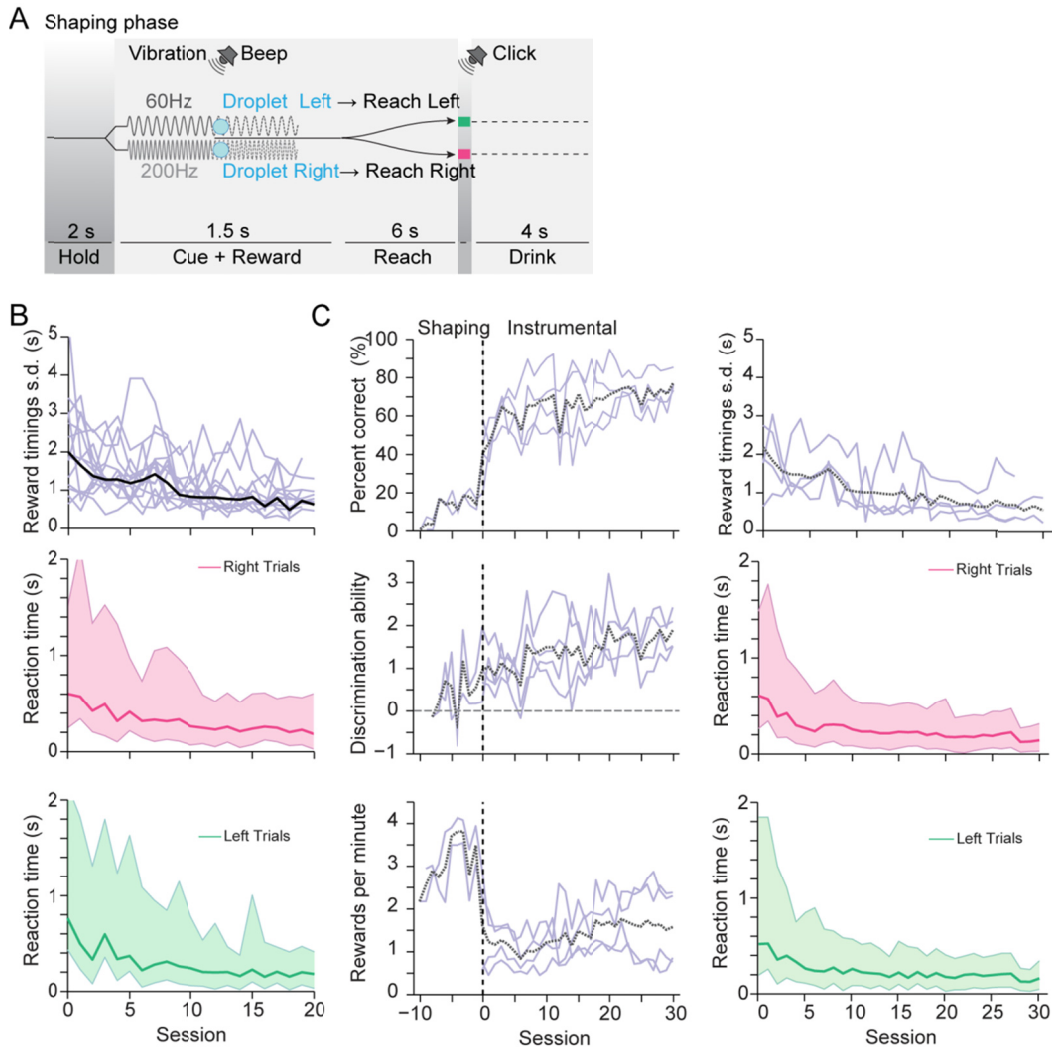
Figure S5. Training of instructed reaching task. Related to Figure 5. (A) Schematics of the training structure during the handling period (shaping phase) showing the sequence of events in a trial. During this phase, mice were not forced to perform instrumental reaches in order to get a reward. After 0.6-1 s of the beginning of the vibratory cue the "go" cue was played and the reward was delivered (60 Hz → left target, 200 Hz → right target) to induce reaching for water movements to the correct target. Mice were then allowed to reach during a time window of 6 s before a new trial started. If mice reached to the correct target within this time, a "click" sound was played and mice were allowed 4 s to drink. As training progressed, the reward delivery was gradually delayed respect to the "go" cue. Under these circumstances mice were able to perform anticipated reaches (i.e. reaching before the droplet was delivered). When anticipated reaches surpassed ~20-30 % of the trials, the shaping phase of the training was finished. (B) Reward timings dispersion and reaction time across sessions of mice depicted in Figure 5G-I to show the distribution of the data. Black trace in reward timings is the mean of 14 mice (light traces individual animals). Pink and green solid lines are the median of the population reaction time; shaded areas cover the 10-90 % quantiles of the distribution. (C) Learning curves of a subset of mice that were trained more extensively than 20 sessions showing not major improvements in behavior.